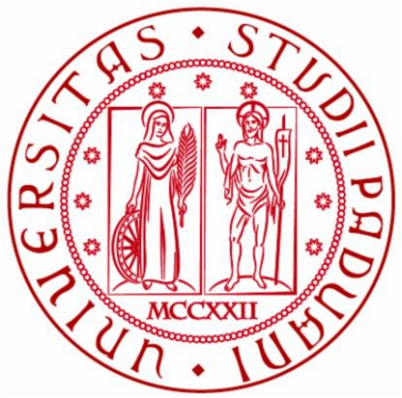

University of Padova
Department of Information Engineering

Master's Degree Thesis in

Bioengineering

Neural Markers of Physiological Modulations Identified with Spectral Analysis of the Vagus Nerve Activity

Supervisor
Gianna Maria Toffolo

Tutors
Alberto Mazzoni
Fabio Vallone

Candidate
Luca Giangreco

Academic Year 2018/2019

Abstract

AIM OF THE WORK

The aim of the present work was to identify modulations in the neural activity of the vagus nerve due to the cardiocirculatory and respiratory alterations. This work could represent a starting point for the decoding of neural activity modulations in the autonomous nervous system and the long-term goal of developing a closed loop device to treat metabolic diseases through nerve stimulation.

Bioelectronic medicine is a new branch of standard medicine whose aim is to treat illnesses like heart failure, epilepsy or diabetes with the use of electrical stimuli instead of drugs. However, to completely understand how to use it, an advanced knowledge of how the nervous system works is needed. One of the most versatile nerves in our body is the vagus nerve (VN) that, given its connection to many organs, is an ideal candidate for bioelectronic medicine studies. Since 1997, when the US Food and Drug Administration (FDA) approved the use of VN stimulation as an adjunctive therapy in the treatment of medically intractable partial epilepsy, the interest on this nerve has continued to increase. Recently, some research groups started to stimulate the VN to obtain heart rate (HR), blood pressure (BP) and respiratory rate (RR) regulation in rats or physiological marker for blood pressure (BPs) and respiratory signals (Rs), by using epineural electrodes (CUFF). However, we still have to understand what is the effect that these physiological alterations evoke in the neural activity. In particular, being able to decode the condition of the patients from VN neural activity will enable us to develop closed loop stimulations. Here we investigated neural activity modulations caused by the application of three types of challenges: increment of blood pressure through infusion of Angiotensin II, increment of the tidal volume (TV) and increment of the respiratory rate. Each challenge showed a significative modulation of the neural activity in the 5-40 Hz range due to stimulation, both in recordings with SELINE and CUFF electrodes. Furthermore, especially for SELINE, not all the recorded channels showed these modulations, thus implying a high recording selectivity of the electrode. Moreover, the histological analysis of the vagus nerve showed a certain organization of its fascicles at the cervical level that could allow identifying the fibers in which the interested signal was transmitted. In conclusion, our results

highlighted how cardiocirculatory and respiratory alterations can affect the neural activity of the vagus nerve and consequently of the autonomic nervous system and pave the way for the development of algorithms able to decode the subject's condition from the VN.

INDEX

Figure index

Table index

1. INTRODUCTION

1.1 BIOELECTRONIC MEDICINE

Bioelectronic medicine is a new field of research that combines the competences coming from the different sectors of bioengineering, neuroengineering, molecular medicine and many others. It appears to be a valid alternative to current pharmacological treatments, used for chronic disorders such as diabetes or hypertension, replacing them with electrical stimulations applied to the nervous system in a targeted manner [1].

The ultimate goal of bioelectronic medicine is the creation of implantable devices at the nervous level, with particular regard to the autonomic nervous system. These devices should allow to decode the signal transmitted by the individual fibers, to verify if this signal corresponds to a normal or anomalous state, caused by diseases or chronic disorders, and finally to modulate it by stimulating or blocking the neural activity in order to restore health [2].

Obtaining a structural and functional biological map of the nervous system is one of the fundamental phases necessary for the development of bioelectronic medicine [3]. It is indeed necessary to be able to establish the intra- and interspecies variations of organ innervation and therefore to build a detailed map for each organ in the most appropriate animal model. As a second step it is necessary to establish the therapeutic feasibility. It is necessary to evaluate, through recording experiments and through stimulation and blocking experiments of neural activity, which are the most appropriate sites and methods to apply, evaluate the correlation between neural signal and biomarkers trend during anomalous states and the effects of neuromodulation. The last phase is that of miniaturization of neural interfaces. It is necessary to adapt the dimensions of the neural interfaces based on the size of the nerves on which they will be applied, also going to investigate new possible materials and structures that could better respond to the structural demands of the nerves. The neural interfaces currently in use are in fact interacting with a large number of fascicles, without distinction [2] [3].

Studies conducted on animal models show the feasibility of the use of neural stimulation to interact with different functions and organs, allowing for treatment of diseases. For example, the work carried out by Koopman et al. [16] show that vagus nerve stimulation inhibits the production of tumor necrosis factor (TNF) and attenuates the severity of rheumatoid arthritis. At the same time studies conducted in humans showed promising results of VN stimulation for treatment of drug resistant epilepsy [12].

In the experimental design of this thesis the physiological and metabolic status of pigs was altered, in particular by modifying their cardiocirculatory, pulmonary and glycemic activities. The neural activity of the vagus nerve, taken at the cervical level, was evaluated and the presence of possible biomarkers that could be used to assess the status of the animals was sought.

1.2 VAGUS NERVE

1.2.1-Autonomic nervous system

The nervous system of vertebrates is subdivided into the Central Nervous System (CNS) and Peripheral Nervous System (PNS) [4]. The latter, consisting mainly of nerves and ganglia, provides the interaction between the body and the central nervous system. The information is transmitted through two categories of nerves. The so-called sensory or afferent nerves take care of the transmission of information from the body to the CNS, and the motor or efferent nerves take care of the transmission from the CNS to the rest of the body. The PNS is in turn divisible between the Somatic Nervous System and the Autonomic Nervous System. The Somatic Nervous System deals with the detection and transmission of information from the external environment to the CNS and the transmission of instructions from the CNS to skeletal muscles. The Autonomic Nervous System (ANS) deals instead with the regulation of involuntary biological functions, such as breathing, heartbeat and metabolism, mainly through feedback mechanisms, allowing the maintenance of homeostasis.

The three subdivisions of the ANS are: Sympathetic (SNS), Parasympathetic (PSNS) and Enteric (ENS). The latter consists of a network of neurons on the gut walls [5]. The peripheral segment of the Autonomic Nervous System consists of a chain of two neurons that connect the CNS to the effector organs. Myelinated preganglionic neurons that form synapses with unmyelinated postganglionic neurons within the ganglia, which, if belonging to the SNS, lie close to the vertebral column, while, if belonging to the PSNS, lie close to the effector organs [7]. Through these chains, most of the automatically regulated organs receive innervations from the sympathetic and parasympathetic divisions of the ANS, with a division that is excitatory, while the other is inhibitory.

These two divisions are complementary and work alternately [6]. Normally the increase of the activity of one of these divisions leads to the reduction of the activity of the other. In general, the PSNS regulates the visceral organs of the head and body cavities (pelvis, abdomen and chest), while the SNS regulates the visceral structures in the body walls and extremities (blood vessels, arrector pili muscle and sweat glands) as well as the organs regulated by the PSNS [5].

The preganglionic neurons of the PSNS flow into the cranial and sacral parasympathetic nerves. Cranial parasympathetic preganglionic neurons originate from different nuclei located in the brain stem, while those of the sacral parasympathetic nerves arise from the intermediolateral regions of segments S2 to S4 of the spinal cord. The cranial fibers of the PSNS are carried by the oculomotor, facial, glossopharyngeal and vagus nerves. These nerves supply fibers from the parasympathetic nervous system to the head, neck, thorax and abdomen. The sacral parasympathetic nerves instead supply fibers to the organs of the pelvis (Figure 1).

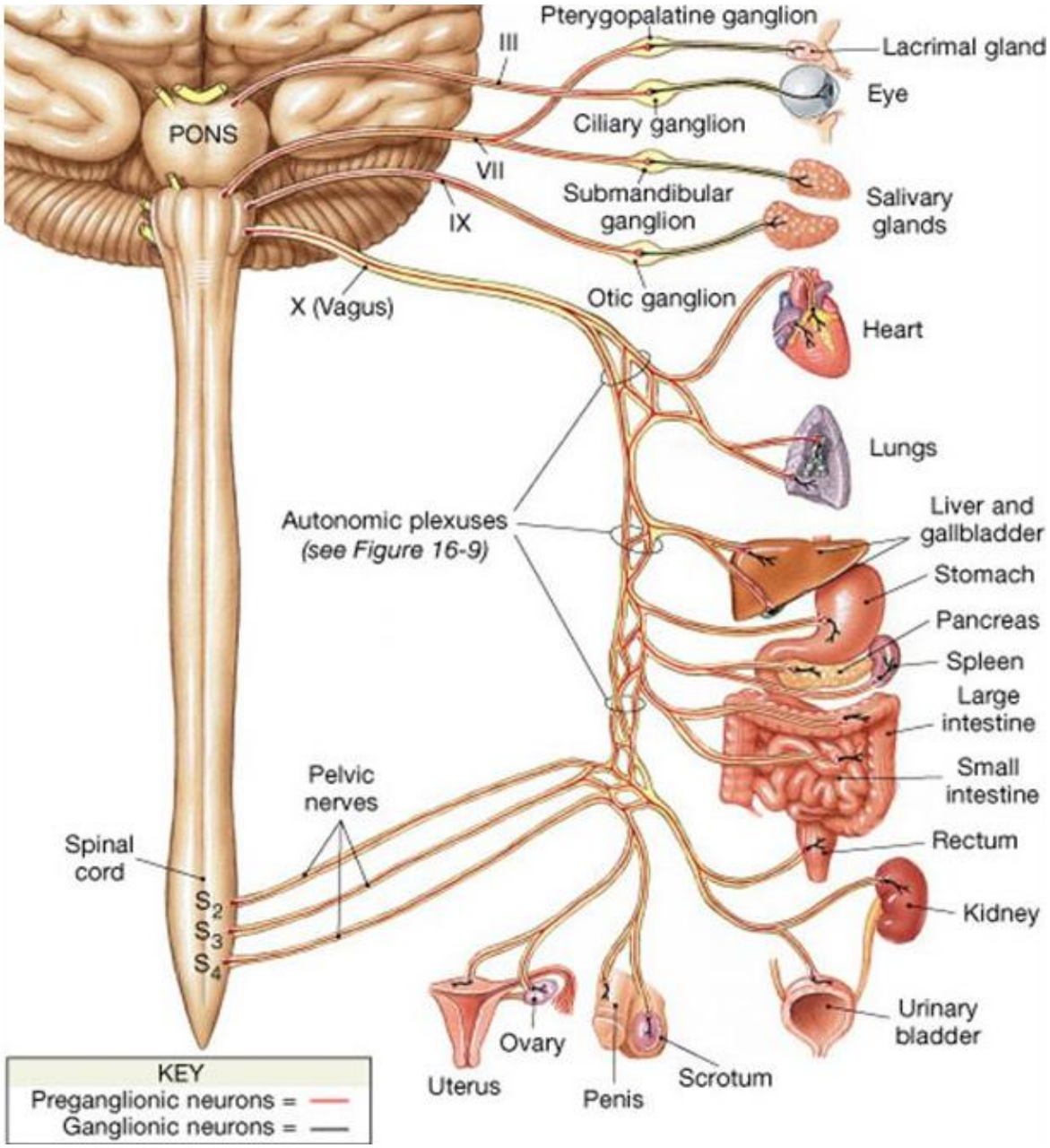

Figure 1: Parasympathetic pathways from [4]

Post-ganglionic PSNS neurons associated with the cranial nerves that supply the head and neck lie in distinct ganglia. While those that supply the viscera in the body cavities are not grouped in macroscopic ganglia, but rather are located both in the nerve plexuses that surround the organ (for example the urinary bladder), and in the gut walls, associated with the enteric nervous system.

The cranial nerves are symmetrical respectively to the cerebrospinal axis. The 12 pairs of cranial nerves were named and numbered in 1664 by Thomas Willis (Table 1) starting

from the anterior to posterior area depending on their shape (Trigeminal), their destination (Facial, Glossopharyngeal) or function (Olfactory, Optic, Auditory) [6].

The PSNS and in particular the cranial nerves, provide the sensory and motor innervations of the head and neck, with the exception of the vagus nerve (see 1.2.2) which also innervates the thorax and abdomen. In addition, some cranial nerves transmit sensory information from the sensory organs. The entire cranial nerve system contains both motor and sensory components and individually the nerves can be purely sensory, purely motor or both.

Table 1: Nomenclature of cranial nerves from [6]

New nomenclature	**Old nomenclature**	**Anatomical name**
Olfactory nerve (I)		N. olfactorii
Optic nerve (II)		N. opticus
Oculomotor nerve (III)	Common ocular motor	N. oculomotorius
Trochlear nerve (IV)	Pathetic nerve	N. trochlearis
Trigeminal nerve (V)		N. trigeminus
Abducent nerve (VI)	External ocular motor nerve	N. abducens
Facial nerve (VII)		N. facialis
Vestibulocochlear nerve (VIII)	Acoustic nerve	N. vestibulocochlearis
Glossopharyngeal nerve (IX)		N. glossopharyngeus
Vagus nerve (X)	Pneumogastric nerve	N. vagus
Accessory nerve (XI)	Spinal nerve	N. accessories
Hypoglossal nerve (XII)	Greater hypoglossal nerve	N. hypoglossus

1.2.2-Anatomy and function of the vagus nerve

Among the cranial nerves, mentioned in the previous paragraph, of particular relevance for bioelectronic medicine is the vagus nerve (X cranial nerve). This nerve in fact performs sensory and motor functions of the head and neck, as well as functions related to the thoracic and abdominal area of the body, going to innervate organs such as the heart, lungs and stomach. The vagus nerve originates in the medulla oblongata and passes through the jugular foramen where it presents an enlargement called upper ganglion or

jugular ganglion. After passing through the jugular foramen, it has a second enlargement called the lower ganglion or plexiform ganglion. In their course between the cervical, thoracic and abdominal level, the right and left vagus nerves have different branches [6]. At the level of the neck they form the meningeal branch, the auricular branch, the pharyngeal branch, the carotid sinus branch, the superior and inferior laryngeal nerves, as well as the cardiac branch, which, proceeding together with the internal carotid artery and the common carotid artery will reach the carotid plexus. At the thoracic level the vagus nerve is distributed in the two pulmonary and esophageal branches, which in turn will go to make up the homonymous plexuses. In this area the two vagus nerves form different branches that exchange fibers with each other and with the sympathetic trunk. These branches will subsequently innervate the trachea, esophagus, pericardium and lungs. Finally, at the abdominal level the vagus nerve goes to innervate organs such as the stomach, liver, pancreas, small intestine and others.

The vagus nerve is the major contributor to PSNS by transporting about 75% of the nerve fibers that constitute it [5]. The neurons contained in it are mixed, with a prevalence of afferents (between 80% and 90%). Its functions can be divided into 3 categories: motor, sensory and autonomous. The motor functions are related to the innervation of the muscles of the pharynx, the soft palate and the larynx where the vagus nerve acts respectively to control the swallowing reflex, prevention of reflux of fluids in the nose and innervation of the motor muscles of the vocal cords. The sensory functions mainly concern the auditory apparatus which is innervated by some branches of the vagus nerve. Finally, of greater importance for the study carried out here, there are autonomous functions. The vagus nerve is responsible for regulating the functions of internal organs, such as digestion, heart rate, respiratory rate, as well as vasomotor activity and some reflexes [9], including functions related to the inflammatory reflex [8].

1.2.3 Peripheral nerve interface

The work carried out during this last years in the fields of implantable electronics and microelectronics allow to develop different types of electrodes able to interface with our nervous system. These devices can be classified in term of their invasiveness or their selectivity. A greater invasiveness is required to obtain a higher selectivity and is connected with the degree of damage produced on the nerve [37].

Peripheral nerve electrodes can be subdivided in three categories [38]: surface electrodes (CUFF or FINE), penetrating electrodes (LIFE, TIME and SELINE) or regenerative electrodes (SIEVE, here not discussed). Here are briefly described the characteristics of these electrodes, following a growing invasiveness order. In Figure 2 is shown a schematic representation of a nerve implanted with CUFF (A), LIFE (B) or TIME (C) electrodes. The hatched area represents the predicted areas of activation during electrical stimulation.

Surface electrodes, such CUFF or FINE (Flat-Interface Nerve Electrode), are wrapped around the outermost membrane of the nerve, the epineurium. They have active sites positioned on the inner surface that came in contact with it and allow the recording and the stimulation of the nerve activity. They are characterized by an easier implantation procedure and a less probability of nerve damage. Compared to intrafascicular electrodes, they have less invasiveness, this ensure a greater longevity [38]. It is difficult to achieve highly selective recording from individual fascicles with these electrodes. But with the use different methodology, like the reshape of the nerve as for FINE or the use of several small CUFF electrodes, it can be achieved.

Penetrating or intraneural electrodes, such as LIFE (Longitudinal Intra-Fascicular Electrode), TIME (Transverse Intrafascicular Multichannel Electrodes) or SELINE (self-opening intrafascicular neural interface), interface with the inner fascicle of the nerve. Compared with extraneural electrodes they have a higher invasiveness but allow a higher selectivity and a lower intensity current is needed for stimulation. According to clinical application they can be implanted in different configurations. Implant is made through the use of a driving wire which allows the positioning of the active sites of the electrode at the desired portion of the nerve. LIFE electrodes are implanted longitudinally to the fascicles, while TIME and SELINE are implanted transversally. With regard to recording performances, an increase of signal-to-noise ratio has been observed when compared to extraneural electrodes [37].

In literature, the most used electrode for recording and stimulation of the vagus nerve activity is CUFF [13] [14] [15], but some paper [20] show how intrafascicular electrodes can be used to reproduce similar results.

In our work we use two type of electrodes, SELINE and CUFF, that are briefly described in 2.1.5.

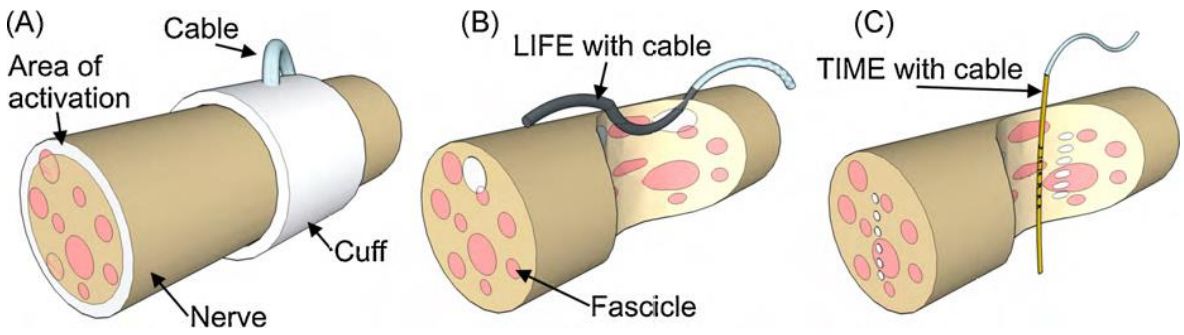

Figure 2: Representations of nerve implanted with CUFF (A), LIFE (B) or TIME (C) electrodes from [39]

1.2.4-Vagus nerve in neuroengineering

Thanks to its different functions, the vagus nerve is therefore of particular interest in neuroscience and bioelectronic medicine. Several studies carried out on animal models have shown that interaction with this nerve can be very useful for understanding and treating diseases such as hypertension [10], sepsis [8], chronic depression, inflammatory bowel disease [9] and epilepsy [11]. For the latter it is to mention the fact that in 1997 the FDA approved the use of vagal stimulation as a treatment method for patients suffering from refractory epilepsy [12]. Through the study of the neural signal transmitted by the vagus nerve it is possible to identify neural biomarkers that allow monitoring of the status and functioning of blood pressure [13] and of the lungs [14]. It has been observed that electrical stimulation of the vagus nerve can cause a decrease in both blood pressure and heart rate [15]. This effect is of particular interest for the treatment of refractory hypertension, for which the pharmacological treatment is not sufficient to bring the blood pressure back to normal levels. It is also possible to influence the functions related to the inflammatory reflex. For example, it has been observed that, again through vagal stimulation, it is possible to inhibit the production of TNF (Tumor Necrosis Factor), an inflammatory molecule found in rheumatoid arthritis. This inhibition leads to a reduction in the severity of the disease [16].

As has been said, all these studies, with the exception of epilepsy treatments, are still under experimentation. It is still necessary to verify, based on the specific organ that we want to analyze, which are the most suitable animal models, types of implants, sites and analysis methods to use. It should however be remembered that the neural interfaces currently in use are interfacing with a high number of nerve fibers, without distinction on

the role played or on the information transmitted [2] [3]. This turns out to be an extremely important factor in studies that include nerve stimulation, as it results in the risk of producing adverse effects.

1.2.5-Vagus nerve in the pig

As has been said, one of the parameters that bioelectronic medicine must take into consideration is the choice of the most appropriate animal model, with reference to the organ of interest. Over the past few decades, the various research groups have begun to work on methods of use and stimulation of the signal transmitted by the vagus nerve in different animal models, including pigs. For this particular animal model, the results obtained mainly concern the cardio-circulatory system and the respiratory system. Some studies, instead, aim to verify the nerve response when subjected to electrical stimuli [17] [18] [19], characterizing the evoked action potentials according to the type of fiber that transports them.

In the works of C. Sevcencu, T. N. Nielsen and J. J. Struijk [13] [14] [20] [21], performed on pigs, is shown the possibility of using CUFF electrodes [13] [14] and intraneural electrodes [20] to derive neural biomarkers, named BPnPs (Blood Pressure neural Profiles) and RnPs (Respiratory neural Profiles). These markers are obtained by a method of average of the power of the filtered neural signal. These two markers, as their name implies, represent the profiles of the two, blood pressure and respiratory cycle signals and can be useful for monitoring the physiological parameters they contain. According to what reported in [20], these two signals are the result of the sum of the single action potentials of the ABR fibers (aortic baroreceptors) and PSR (pulmonary stretch receptors), respectively for the BPnP and the RnP, and therefore are dependent by the frequency of activation of these fibers. These two neural markers could be useful for the treatment of refractory hypertension. In a close loop mechanism, through the electrode implanted on the vagus nerve, one could proceed to estimate these markers and the relative physiological parameters, in real time. Subsequently, in the event of a state of hypertension, nerve stimulation could be performed using electrical impulses, thus modulating the transmitted signal. It has already been verified, although mainly in mice, that stimulation of the vagus nerve can result in an activation of the ABR fibers and a consequent decrease in blood pressure [10] [15] [22]. While the BPnP marker would act as a trigger for the

activation and deactivation of neural stimulation, the RnP marker would act as a control mechanism, to prevent the activation of the stimulation in the cases it is not necessary. For example, during the performance of physical exercise, which would lead to an increase in blood pressure that would not require the intervention of vagal stimulation, since it is not caused by anomalous situations. In this situation, the RnP marker, verifying that an intensification of pulmonary activity occurs at the same time as the increase in blood pressure, would prevent the activation of the stimulation.

1.3 VAGUS NERVE BIOMARKERS AND NEUROMODULATION

1.3.1-Pressure marker

As mentioned in the previous paragraph, 1.2.4, the signal transmitted by the vagus nerve can be used to derive neural markers of physiological parameters. Here it will be shown the use of this signal to obtain pressure markers, i. e. markers that can provide information regarding physiological parameters such as systolic pressure, diastolic pressure and mean pressure. Recent studies carried out by Sevcencu et al. [13] and reported by T. P. Zanos [23], aim to investigate for the presence of a possible pressure marker using implanted tripolar cuff electrodes on the vagus nerve. These studies were performed on a total of seventeen anesthetized pigs, in which two cuff electrodes, 5-7 cm apart, were implanted in the left vagus. Arterial blood pressure was measured by implanting a catheter in the right carotid artery. An increase in blood pressure was induced, after a baseline period of 5 minutes, by adrenaline administration. In ten pigs the blood pressure level was increased three consecutive times, alternated by short periods in which the level was kept constant. The ECG signal was recorded during the course of the experiments and the R peak was used as reference for an ensemble average of the neural signal and of the blood pressure signal. Squaring the appropriately filtered neural signal provided the blood pressure–related neural profile (fig. 2). Neural related and blood pressure signals were morphologically identical, with the pressure signal preceded by about 40 ms from the neural signal. It is hypothesized that this delay is due to the separation (8-10 cm) between the catheter of the carotid arterial pressure and the cuff electrode of the vagus nerve. Systolic, diastolic, and mean pressure levels were

shown to be linearly correlated with the related neural profiles. To conclude, the neural origin as well as the afferent origin of the recorded signal was verified by vagotomy.

Figure 3 presents the results provided by Sevcencu et al. [13]. It is possible to note the mentioned gap between the BP signal and the BPnP signal, evidenced by the double arrow in the first panel, as well as the presence of the two systolic peaks (P1, P2, nP1 and nP2) and of the dicrotic wave (DW and nDW). The data presented are related to the second animal (first injection in the upper left panel and second injection in the upper right), third animal in the lower left panel and fourth animal in the last panel.

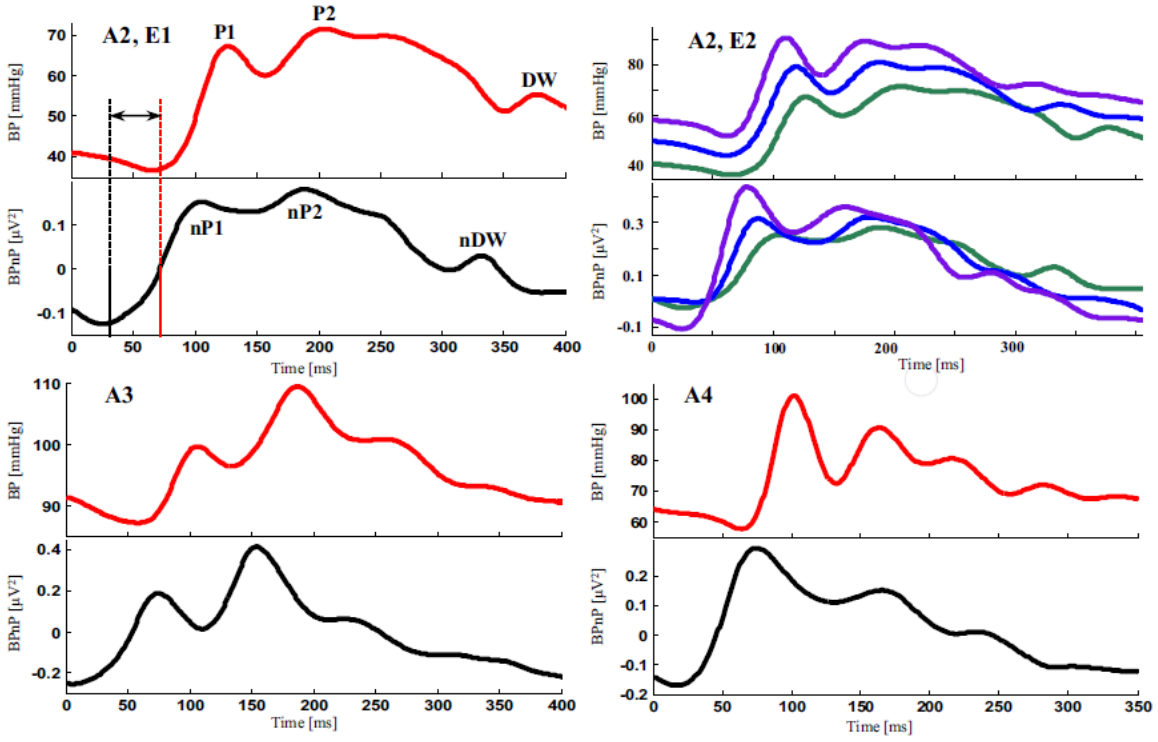

Figure 3: comparison between BP and BPnP signals from [13]. First and second panel compare the same animals (A2) in the two experiments, single (E1) and multiple(E2) bolus of Adrenaline. Third and fourth panel refer to respectively animal A3 and A4.

Other studies carried out to investigate the effects of vagal stimulation on the control of blood pressure have been carried out by Platcha et al. [15].

1.3.2-Respiratory marker

Another type of neural marker useful for the treatment of diseases such as refractory hypertension is the respiratory marker. Studies such as those presented in 1.3.1 have

been carried out by Sevcencu et al. [14] and reported by T. P. Zanos [23], concerning the possibility of using the neural signal transmitted by the left vagus nerve to obtain a marker related to the respiratory cycle (RC). As reported by T. P. Zanos in [24] the signal transmitted on the left vagus nerve would contain information related to respiratory activity. The experiments of Sevcencu et al. [14] were performed on anesthetized pigs. Five were subjected to changes in respiratory rate, while nine were subjected to changes in respiratory volume. As for the study of the pressure marker, the activity of the left vagus nerve was recorded using two cuff electrodes. The respiratory cycles were instead monitored through the use of a pressure transducer. Squaring the appropriately filtered neural signal provided the respiratory related neural profile (fig. 3).

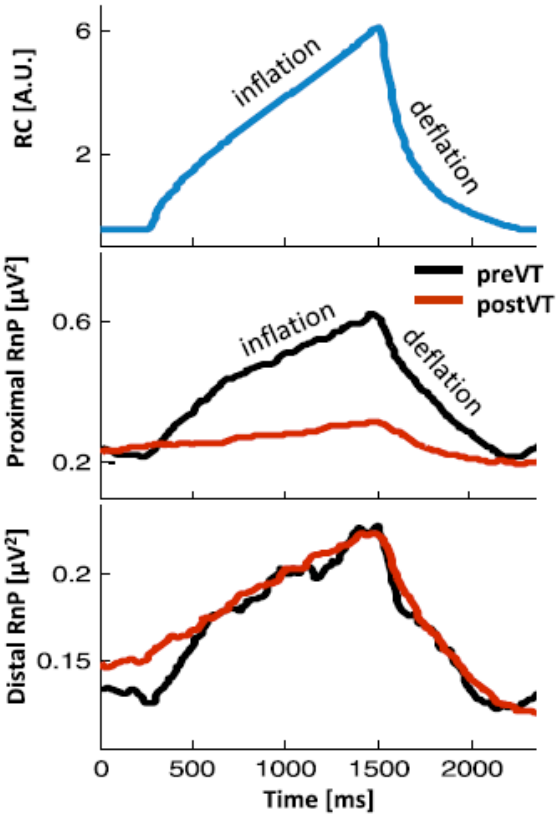

Figure 4: Comparison between respiratory cycle (RC, first panel) and respiratory related neural profile (RnP) extracted from proximal (second panel) and distal (third panel) CUFF electrodes pre and post vagotomy (preVT, postVT) from [14].

Also in this case, the RnP was morphologically similar to the respiratory cycle. In terms of duration and amplitude of the components of inflation and deflation of respiratory activity, the respiratory related neural profile showed a significant linear correlation with

the respiratory signal. Finally, the vagotomy procedure was performed in the area between the two electrodes to verify that the recorded activity was neural and if it was due to afferent or efferent components. Being that after the vagotomy, the respiratory related neural profile has almost completely disappeared on the proximal electrode, but remained unchanged on the distal electrode, it is possible to state that the recorded activity, not only is neural, but more precisely comes from afferent fibers.

In Figure 4 are shown the trends of the respiratory cycle signals (in the upper panel), of the respiratory related neural profile taken from the proximal electrode, pre and post vagotomy (central panel) and of the respiratory related neural profile taken from the distal electrode, pre and post vagotomy (lower panel).

Results similar to those shown in Figure 3 and Figure 4, relative to the two markers BPnP and RnP, were obtained from Sevcencu et al. [20] through the use of a custom-made intraneural electrode.

1.3.3-As a treatment for epilepsy

In 1997, the US Food and Drug Administration (FDA) approved vagus nerve stimulation (VNS) as adjunctive therapy for reducing the frequency of seizures in patients >12 years of age with partial-onset seizures refractory to antiepileptic medications [12]. Research on studies carried out between 1999 and 2012 on the effect of vagus nerve stimulation on patients suffering from epilepsy, carried out by George L. Morris III et al. [25], reports that this treatment has occurred to be effective. In particular, vagus nerve stimulation is associated with a >50% seizures reduction in 55% of 470 children with partial or generalized epilepsy, in sixteen studies. Reporting that vagus nerve stimulation may be considered as adjunctive treatment for children with partial or generalized epilepsy and may be considered a possibly effective option after a child with medication-resistant epilepsy has been declared a poor surgical candidate or has had unsuccessful surgery. In this research they state, as a recommendation, that vagus nerve stimulation could also be used for patient that suffer for seizures associated with Lennox-Gastaut syndrome. They report that in four study carried out on a total of 113 patients, vagus nerve stimulation is possibly effective in achieving >50% seizures frequency reduction in 55% of the patients, similarly to the response rate of children with partial or generalized epilepsy. Other

conclusions were reported, concerning the use of vagus nerve stimulation to improve the mood in patients with epilepsy and the reduction of seizures frequency over time. For the latter is stated that vagus nerve stimulation in possibly associated with an increase in ≥50% seizure frequency reduction rates of 7% from 1 to 5 years post implantation.

1.3.4-Other

As the preceding paragraphs show, the neural signal transmitted by the vagus nerve could be used to derive neural biomarkers, which would allow us to obtain information on the health status of the animals. Or be modulated through the use of electrical impulses in order to treat and decrease the effects of chronic diseases such as refractory hypertension or refractory epilepsy, otherwise not treatable with existing drugs. However, those shown above are not the only uses of this signal. In fact, it has been observed that the activity of the vagal afferent fibers is linked to changes in the glycemic level [27]. Other studies have shown instead that the production of cytokines is related to the activity of the vagus nerve [24] [26] and how this can be inhibited through the use of electrical stimuli applied to it [8] [16]. These studies focused on two particular types of cytokines, interleukin 1β (IL-1β) and tumor necrosis factor (TNF). These two cytokines are produced by macrophages and released from the intestinal mucosa during inflammatory events [9]. Given their role in the mechanisms of the inflammatory reflex, the inhibition or stimulation of these cytokines by stimulation of the vagus nerve can be useful for the treatment of diseases such as rheumatoid arthritis or inflammatory bowel diseases.

2 Materials and methods

The following experiment were carried out in nine session at the CNR (Consiglio Nazionale delle Ricerche) area of Pisa in the laboratory of Prof. Fabio Recchia of the Institute of Life Sciences of Scuola Superiore Sant'Anna, with the collaborations of colleagues of the Scuola Superiore Sant'Anna.

2.1. Experimental setup

2.1.1-Animal model

A total of 9 farm pigs of weight around 30 Kg was subject to the experimental procedure. It was decided to study the behavior of the neural signal of the vagus nerve when the animals undergo to changes in the physiological and metabolic state. Challenges were therefore carried out to increase the Respiratory Rate (RR) on 7 pigs and increase the Tidal Volume (TV) on 9. The challenges of infusion of Angiotensin II (AII) were performed on 9 pigs and those of infusion of Sodium Nitroprussiate on 2, to obtain respectively an increase and a decrease in the level of blood pressure. Glucose infusion and insulin injection challenges were performed on 3 and 2 pigs respectively. In four of the pigs the neural activity was recorded from the left vagus nerve at cervical level, while for the other five the activity was recorded from the right vagus nerve. Two type of electrode were used for the recording, SELINE electrode and cuff electrode. In particular, SELINE electrodes were used on 6 of the total number of animals, while cuff electrode on the remaining 3. Cuff electrode was used even for stimulation of the vagal activity in order to compare our results with literature.

2.1.2-Animal preparation

On all the animals was carried out the same procedure, here exposed:

Pigs were fasted from the night before the experiment. In the morning they were anesthetized with the use of a first injection of propofol, followed by a continue infusion of isoflurane during the experiment to allow the maintenance of the anesthetized state. After this, we proceeded with the connection of the animals with the devices for the ECG

and blood pressure monitoring, Leycom Sigma 5/DF and HP Viridia 24c. The BP signal was taken from the femoral artery.

The animals were then intubated and connected with the device Servo Ventilator 900c for the monitoring and control of the respiratory activity, in particular the respiratory rate and the tidal volume.

Last, an access to the recording site has been created through the incision of the frontal area of the neck. The nerve has been separated from the carotid artery and the rest of the pigs for a length of 7-10 cm. In this area the electrodes were inserted, always trying, in the case of SELINE electrode, to insert it transversally to the nerve along the vertical axis perpendicular to the longitudinal axis.

The challenges were carried out with a randomized order, in the way of avoiding possible plasticity phenomena of the physiological and metabolic state.

At the end of the experiment the animals were sacrificed and the left and right vagus nerve were extracted for a subsequent histological analysis.

2.1.3-Challenge

During the experiments, alterations of the physiologic and metabolic state were imposed to the animals in order to search for variation of the electrical activity of the recorded signal.

We decided to work with 3 types of alteration of the physiologic and metabolic state:

- Alteration of the respiratory activity
- Alteration of the cardio-circulatory activity
- Alteration of the glycemic level

It has also decided to carry out some secondary challenge of electrical stimulation during the experiments that involved the use of CUFF electrodes to obtain a comparison with the results present in literature. Stimuli were imposed with a Duty Cycle of 50% and Pulse Width of 400μs.

The challenge requires to perform stimulations on the vagus nerve by altering the two stimulus parameters, amplitude and frequency, with the following values (Table 2). Every possible combination has been tested.

Table 2: List of parameters used for the stimulation

Amplitude (mA)	1	1.5	2	2.5
Frequency (Hz)	10	20	30	40

2.1.3.1-Respiratory

The variation of the respiratory activity was imposed by the use of the device Servo Ventilator 900c.

For the first five experiments to the animals was imposed an initial Respiratory Rate (RR) and Tidal Volume (TV) respectively of 10 act/min and 400cc. This condition was taken as the respiratory baseline. During the different challenges this two parameters have been made to vary singularly, RR was imposed to 15 and 20 act/min, while TV was altered to the values 500, 600 and 800cc. This state was maintained for 2 to 5 minutes during which the nerve activity was recorded.

In the rest of the experiments the baseline and challenge conditions were changed. For the baseline condition were imposed RR to 15 act/min and TV to 450cc, while for the challenges were imposed an RR of 30 act/min and a TV of 900cc.

Below is represented the table of the different combination used with the relative indication of baseline or challenge condition (Table 3).

Table 3: List of parameters for the respiratory challenges

	RR	TV
BASELINE	10/min	400cc
CHALLENGE	15-20/min	400cc
CHALLENGE	10/min	500-600-800cc
BASELINE 2	15/min	450cc
CHALLENGE	30/min	450cc
CHALLENGE	15/min	900cc

2.1.3.2-Cardio-circulatory

Cardio-circulatory challenges were performed by the infusion of Angiotensin II (AII) and Sodium Nitroprussiate, respectively a vasoconstrictor and vasodilator.

The desired effect for AII infusion was an increase of blood pressure and a consequent reduction of the heart rate due to the effect of activation of the baroreceptive reflex. While, an inverse effect, of reduction of the blood pressure and increase of the heart rate was expect for the infusion of Sodium Nitroprussiate. However, in the experimental phase was observed that the HR increase during the infusion of AII and decrease during the infusion of Sodium Nitroprussiate, with a slight delay in respect to the BP trend.

The 3 possible reasons, yet to be verified, are:

- Anesthesia may have acted as a confounding factor and may have prevented the activation of the baroreflex.
- The reached BP value may have been insufficient for the activation of the baroreflex.
- Knowing that AII influence even CNS and in particular the nucleus of the solitary tract, in which converge the vagal afferents, the amount of infused AII, greater than the physiological concentrations, may have inhibit the baroreceptive reflex.

The infusion values imposed for the different pigs vary between 18 and 84 ml/h for AII and 5,4 or 10,8 ml/h for Sodium Nitroprussiate.

2.1.3.3-Glycemic

Glycemic challenges were performed by the infusion of Glucose and injection of insulin. During the challenges the glycemic level was kept under observation by blood samples taken at intervals of 5 minutes, with the use of a glucometer.

Reached a certain glycemic level, this was tried to kept constant for some minutes, after this, pigs were constantly kept under observation, via the monitoring of the glycemic level and no other external action, till the returning into baseline conditions.

The infusion quantity of glucose and insulin injection during the experiments were:

- Glucose: 45-90 ml/h

- Insulin: 1.56 ml

2.1.4-Recording Apparatus: Tdt

The recording apparatus has three principal components: the electrodes, the Tucker Davis Technology (TDT)'s Neurophysiology Workstation RZ5D BioAmp Processor and the PZ5 multichannel amplifier. During the stimulation phase of the experiment another TDT's component, the multichannel stimulator IZ2-MH, was used. All TDT's component can work with frequency up to 50 KHz and with a total amount of 32 channels [28]. Signals were acquired with a sampling frequency of 24 KHz and with a maximum of 16 channels. Physiological signals were directly acquired, while neural signals were filtered using second order Butterworth filters reported in Table 4. After filtering, the signals have been stored to allow off-line analysis.

Table 4:Type and order of application of the filters used during the recording of the neural data

Order of application	Type	Frequency [Hz]
1	Notch	50
2	Notch	100
3	Notch	150
4	High-pass	10
5	Low-pass	5000

Matlab/TDT graphic user interface, shown in Figure 5, together with another interface of the TDT device, here not shown, allow for real time observation of physiological signals and neural signals together with the FFT of the neural signals, evaluated with RZ5D at interval from 1 to 5 seconds, usually 3. Furthermore, this interface allowed for the setting of the parameter of the stimuli used during the stimulation challenge. The GUI consist of an upper part of panels for the settings of the parameters of the stimuli and the setting of which channel would be visualized below and a lower part dedicated to the visualization of the power spectrum. Starting from the left, the first panel allow the choice between recording and preview. Second and third panel, dedicated to the stimuli, respectively allow the choice of the channel in which the stimulation would be done and the setting of the parameters of the stimuli. The parameters that can be set in this last panel are:

- Max Curr (μA): Maximum amplitude of the transmitted current during the stimulus
- Min Curr (μA): Minimum amplitude of the transmitted current during the stimulus
- Curr Step (μA): Amplitude of the step of variation
- Freq: Frequency of the stimulus
- Ratio A1/A2: Ratio between the positive and negative amplitude
- N pulse: Number of pulses sent during the stimulation
- PW1 (μs): Time for which the signal is at high level
- PW2 (μs): Time for which the signal is at low level

The button UPD update the parameters, while the fourth panel with the two buttons Start stim and Stop stim, starts and ends the stimulation. Last panel, dedicated to the visualization, allow three different choice:

- Visualization of all or none of the channels
- Visualization of a subset of all the channels, selecting the first and the last channel to visualize
- Visualization of only one channel

The row below the panels enable the Fourier transform by setting the length of the time window for the evaluation. The Notes panel allow to enter notes regarding the file, these notes were stored in a separated text file.

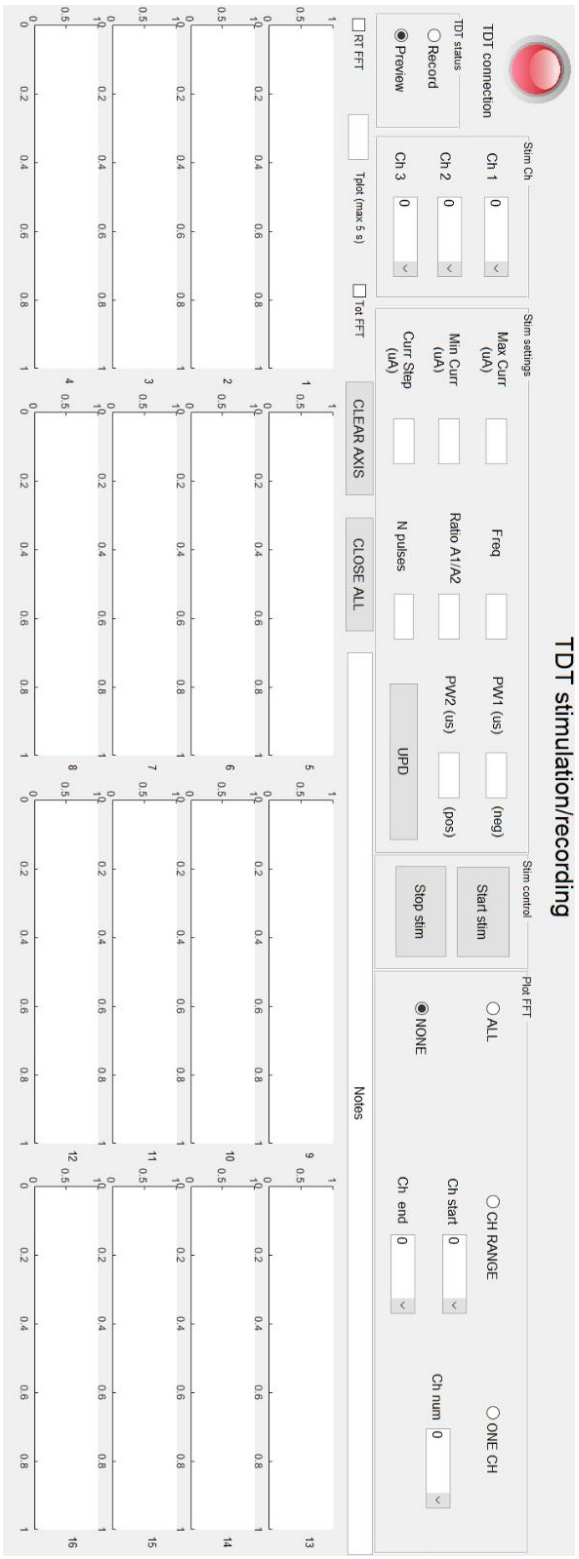

Figure 5: TDT/Matlab GUI

2.1.5 Neural data acquisition

To verify which type of electrode is more suitable for the study of the signal transmitted by the vagus nerve, during the project the signals recorded by CUFF and SELINE electrodes were analyzed. We use one CUFF electrode with three active sites and two SELINE electrodes with respectively 10 and 16 active sites. Here is a brief description of these two types of electrodes:

- **SELINE**

  SELINE electrode is an evolution of TIME's and LIFE's electrodes, its main structure is made of thin films of polyimide, a lightweight, flexible and biocompatible polymer yet widely employed for neural interfaces [40].

  The electrode is made of a symmetric looped structure with wings positioned along the two side of the shaft, as is shown in Figure 6. The apical part of the shaft has a constriction in order to ease the insertion of the electrode and the active sites are positioned both on the shaft and on the wings, two for each wing.

  The working principle is based on the insertion of the electrode inside a hole, previously made by a needle, followed by a partial extraction that allow the opening of the wings. This procedure is suitable for transverse insertion and not recommended for longitudinal implantation, because, in the last case, the force that is needed to be applied for the extraction would be not parallel to the direction of the insertion, bringing difficulties in the opening of the wings.

  In Figure 6 is shown a schematic representation of a SELINE electrode. The looped structure of the shaft allows for the insertion of the needle and wire that are used for the insertion of the electrode inside the nerve. The wings, during the action of partial extraction, opens, anchoring the electrode to the nerve and allowing the active sites positioned on them, to record from different position inside the nerve.

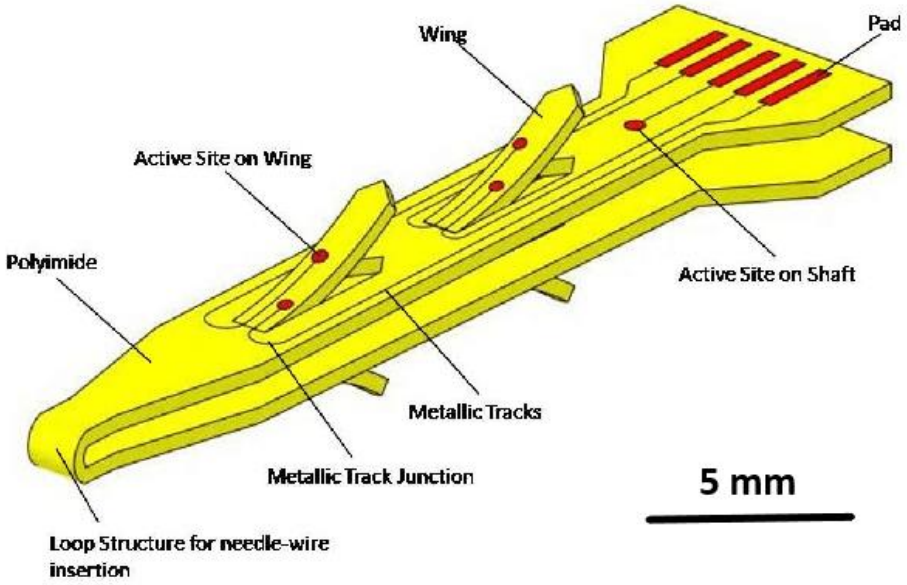

Figure 6: Schematic representation of a SELINE electrode from [40]

- **CUFF**

  CUFF electrodes are made of an insulating layer that encircle the nerve, with two or more active sites on the inner surface that are connected to insulated wires (Figure 7). The two most known are the “split-cylinder” and the “spiral” CUFFs type, the last used during this project. They offer different advantages compare to some of the previously mentioned electrodes type, such the reduction of the stimulus amplitude or the confinement of the stimulating current in the inner space of the electrode. However, they are subject to a low signal-to-noise ratio. For this reason, CUFFs are often used with the bipolar or tripolar configuration, in the latter the central active site is used as cathode and the outer two active sites are used as anodes, reference.

  This strategy was not implemented during this project, to maintain the consistency between the analysis of the data coming from the SELINE electrodes and the one coming from CUFF.

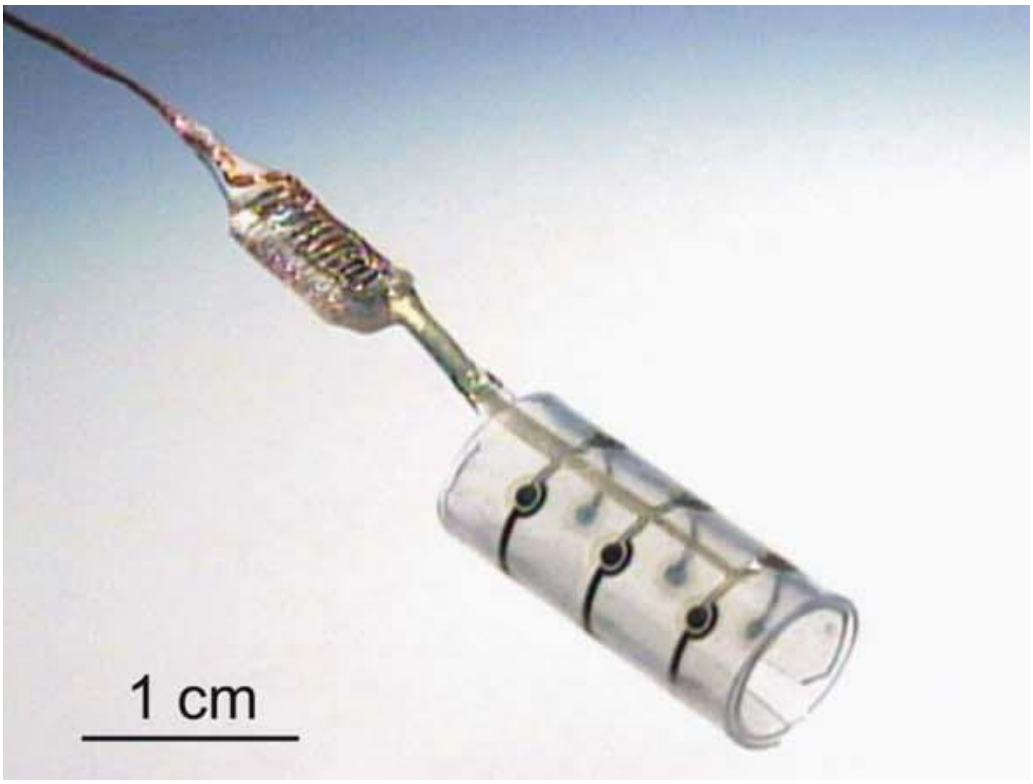

Figure 7: CUFF electrode used in for PNS activity recording and stimulation from [41]

2.2 Data analysis

2.2.1-Theoretical foundation

Data analysis carried out during this thesis make use of two principal methods: the estimation of the correlation coefficient between the data coming from different channels of the same recording and the evaluation of the power spectral density (PSD) through the use of Welch power spectral density estimation. Here we discuss about the theoretical foundation of these two methods.

- Correlation coefficient:

  The correlation coefficients of two variables indicate the degree of linear dependence present between them. They can take values between -1 and +1 and are calculated using the following formula

$$\rho(A,B) = \frac{1}{N-1}\sum_{i=1}^{N}\overline{\left(\frac{A_\iota - \mu_A}{\sigma_A}\right)}\left(\frac{B_i - \mu_B}{\sigma_B}\right)$$

or alternatively

$$\rho(A,B) = \frac{cov(A,B)}{\sigma_A \sigma_B}$$

where N indicates the number of observations of the variables, μ_A and μ_B indicate their mean value and σ_A and σ_B indicate their standard deviation.

- Welch power spectral density estimation:

  The Welch method is a power spectral density estimation method based on the spectral estimation of the periodogram. The estimation is made by dividing the signal into time segments, X_k, of the same length, usually with overlap between them. Then, given a chosen window W, the sequence of X_k*W is formed and from this the sequence of the finite Fourier transforms $A_k(n)$ is calculated. The modified periodograms, $I_k(f_n)$, are obtained as the ratio of the energy of the Fourier transform over the power of the window. Finally, the estimation of spectral power density, $\hat{P}(f_n)$, is obtained as the average of the modified periodograms [29].

$$A_k(n) = \frac{1}{L}\sum_{j=0}^{L-1} X_k(j) * W(j) * e^{-2kijn/L}$$

$$I_k(f_n) = \frac{L}{U}|A_k(n)|^2$$

$$U = \frac{1}{L}\sum_{j=0}^{L-1} W(j)^2$$

$$\hat{P}(f_n) = \frac{1}{K}\sum_{k=1}^{K} I_k(f_n)$$

  Where j, L and K indicates respectively the time instant, the length of the segments, and the number of segments, while f_n=n/L.

  This procedure allows to obtain a reduction of the variance of the periodogram, but does not provide information on the temporal variations that take place in the spectrum.

2.2.2-Neural data applications

The spectral analysis was implemented through the use of the Matlab command line pwelch. One thing that has to be taken into consideration during the application of this method is the length of the time segment that we want to analyze. After the elimination of the artifacts that affect the signals, see 3.2, the length of the segments goes from 10 to

15 seconds. In order to obtain an adequate estimation of the PSD of the segments, Welch method was applied with a Hamming window of length of 1 second and using an overlap of 50%. In this way the power spectral density was estimated with more than 10 segments.

3 Data Processing

Processing of the signal, made entirely with the use of the software Matlab, was carried out in two steps. The first step was carried out on all the set of data of the different experiments, while, the second step was carried out only on a subset that was classified as significative.

During pre-processing the physiological signals were first filtered and some physiological parameter were extracted. These parameters were used for checking the condition of the animal and for searching an appropriate time segment in which to perform the analysis. The stored neural signals were evaluated in order to search for correlation between the different recorded channel and an observation of the frequency spectrum of the selected time segment was performed in order to evaluate which were the file with more significative variation. The subset of data that present significative variation was then used for the next part of the processing.

The recorded data present two evident types of artifact. During the data analysis of the subset of data these two artifacts were removed and a filter between 5 Hz and 5 KHz was then applied to the different channels. In order to avoid inconsistencies between the amplitudes of the recorded signals, due to the possibility that the active sites were not in full contact with the fascicles, each channel was normalized, subtracting its own average and dividing by its standard deviation (z-score of the signal). The problem of very high correlation between the channels was then solved with the use of a common mode rejection algorithm. At this stage any possible residual artifact was manually removed. Last, to evaluate the variation of the power spectral density, an analysis of the frequency spectrum of the cleared neural signals was carried out.

During the process, every challenge was compared with its previous baseline in order to search for alteration of the neural signals induced by the alteration of the physiologic and metabolic state. All the filters used during the processing were implemented with the use of the Matlab command filtfilt and their coefficient were extracted with the use of the command line butter.

3.1 Pre-processing

The stored data were classified according to the type of challenge applied to the animals. During the pre-processing part, the physiological signals of each challenge file were compared with those of the previous baseline file. In order to do so some physiological parameter need to be extracted. Physiological signals were then filtered with a 10 to 100 Hz pass-band filter for the ECG signal and a low-pass filter with a cut-off frequency of 100 Hz for blood pressure and respiratory cycle signals. The band-pass filter applied to the ECG signal allowed to remove possible drifts caused by respiratory and blood pressure cycles, which have their main frequency components below 10 Hz. Regarding the ECG signal, the applied filter was a sixth order band-pass Butterworth filter between 10 and 100 Hz. Starting from the R peak we were able to evaluate the HR of the animals, in particular we use the evaluated value of the HR in the time course to evaluate the stability of the ECG signals. The R peak of the ECG signal were identified with the use of a thresholding algorithm and then verified by visual inspection. The HR was computed for each R peak (T_p) as the inverse of the interval between two consecutive R peaks multiply by 60, as shown in the following formula. This allowed us to obtain the HR value expressed in Beats Per Minute (BPM).

$$HR[BPM] = \frac{1}{T_{P_i} - T_{P_{i-1}}} * 60$$

A similar process was applied to the respiratory cycle signal in order to obtain the respiratory rate. The respiratory cycle signal has been filtered with a low-pass Butterworth filter of sixth order with a cut-off frequency of 100 Hz. As for the ECG signal a thresholding algorithm was used to detect the inflation peak and verified by visual inspection. The respiratory rate was computed as the inverse of the interval between two inflation peaks multiplied by 60. The second parameter that was extracted from the respiratory cycle signal was the Volume change. This parameter has been computed as the ratio between the mean of the peak-peak of the signal in the challenge file (PP_c) over the mean of the peak-peak of the signal in the baseline file (PP_b). This parameter was evaluated only in the time segment that was chosen for the analysis, so only in the phase where the physiological signals were stable.

$$Volume\ change = \frac{mean(PP_c)}{mean(PP_b)}$$

Last, the blood pressure signal was filtered with the same filter applied to the respiratory cycle signal and was then converted from µV to mmHg with the use of the following linear relation:

$$\frac{V_{sn}}{V_{si}} * BP_{si} = BP_{sn}$$

$$\frac{V_{dn}}{V_{di}} * BP_{di} = BP_{dn}$$

where the index s, d, n, i, are related respectively to systolic, diastolic, nth and initial and the nomenclature V wants to express the fact that the signal was expressed in µV.

From the time course of systolic and diastolic pressures the 3 parameters of mean systolic pressure, mean diastolic pressure and mean arterial pressure (MAP) were extracted. The last one has been extracted both in terms of time course and in terms of average on the entire time interval.

$$MAP_n = \frac{1}{3}BP_{sn} + \frac{1}{3}BP_{dn}$$

Extrapolation of these data allowed analysis of the stability of physiological signals. Later, in fact, we went to select some temporal intervals in which the physiological signals were stable.

In order to understand the degree of selectivity provided by the electrodes it was necessary to go and see the level of correlation between the different channels. The calculated correlation coefficients, as can be seen in Figure 11 in 3.2, showed that the initial correlation level between channels was very high (in general >0.8). To decrease this level of correlation, during the second part of the analysis it was decided to remove the component common to the channels.

As has been previously said, through the extracted physiological parameters and the visualization of the physiological signals, the temporal segments of the files on which the analysis has been carried out have been selected. The conditions to consider these segments as an adequate working zone were:

- Stability or near stability of physiological parameters along the whole segment
- Fewer artifacts visible in the neural signal
- Length of segment between 15 and 60 seconds, normally used 30-second intervals

As last point, we observe the power spectrum of the neural signals in these segments and we select the file for which the change in the low frequency, between 5 and 40 Hz, from baseline to challenge, were more relevant.

In Figure 8 is shown an example of the physiological signals for a selected working zone of a challenge of increase of the RR. Respectively the ECG in A), blood pressure in B) (full circle for diastolic pressure, empty circle for systolic pressure and solid line for mean arterial pressure, MAP), the respiratory activity in C) and the HR in D)

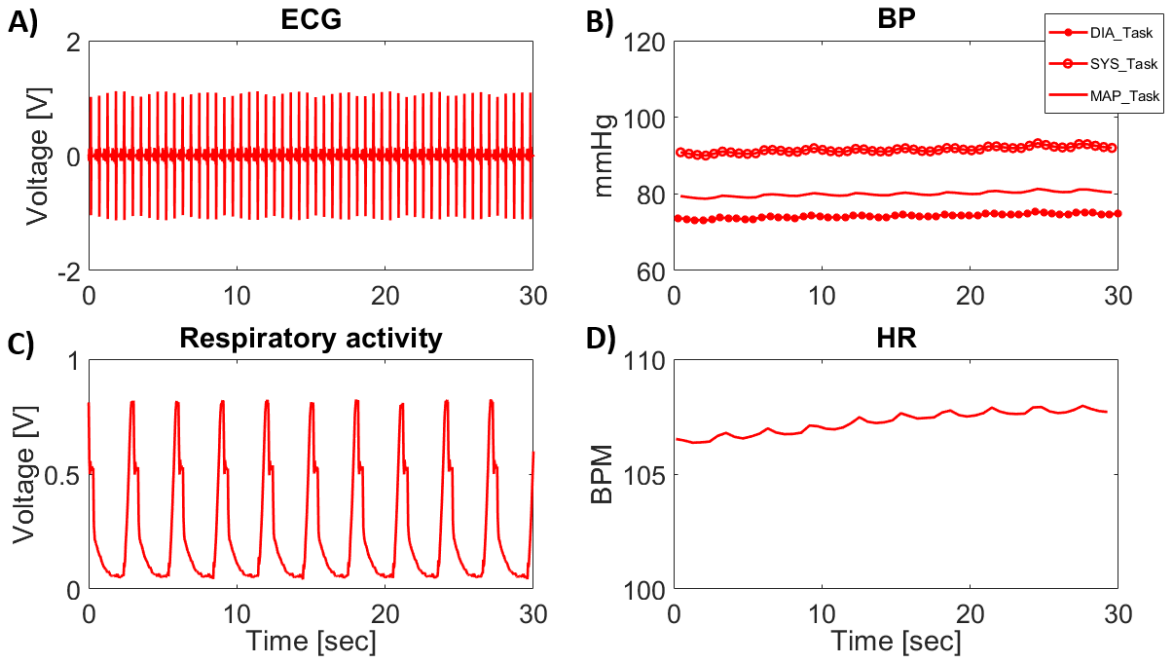

Figure 8: Example of the physiological signals of a selected segment of a challenge. Respectively the time courses of: ECG (A), Blood Pressure (B), Respiratory activity (C) and Heart rate (D).

3.2 Data analysis

The chosen subset of data was analyzed in the time and frequency domain. Two types of artifact were identified during the analysis of the neural signal, cardiac activity related artifacts and peak artifacts. These two artifacts could be more or less evident between the files and between the channels. We proceeded to the elimination of these artifacts through the use of the following procedures:

- **Cardiac activity related artifact**

  This artifact was visible during, or immediately after, the peak of the R wave of the ECG signal. This suggested that it was closely related with cardiac activity or, as a second hypothesis, with the movement of the carotid artery caused by the pulsation trend of the blood flow. We then decide to use a relatively simple procedure for its identification and removal, that make use of this hypothesis. Knowing that the periodicity of the artifact was similar to the one of the ECG signal and that the main frequency component of the latter are located in the range between 10 and 100 Hz. The same filter that was previously applied to the ECG signal was here applied to the neural signals. Then, taking as reference the channel in which this artifact was more recognizable, an automatic search for the minimum values of the filtered signal in proximity of the R wave was started. This allowed us to obtain the mean delay between the R peaks and the artifacts. This delay was than summed to the temporal instants of each of the peaks of the R wave in order to obtain an approximation of the position of the different artifacts along the chosen segment.

  Last, we removed a 300-350 ms time segment around the estimated position of the artifacts.

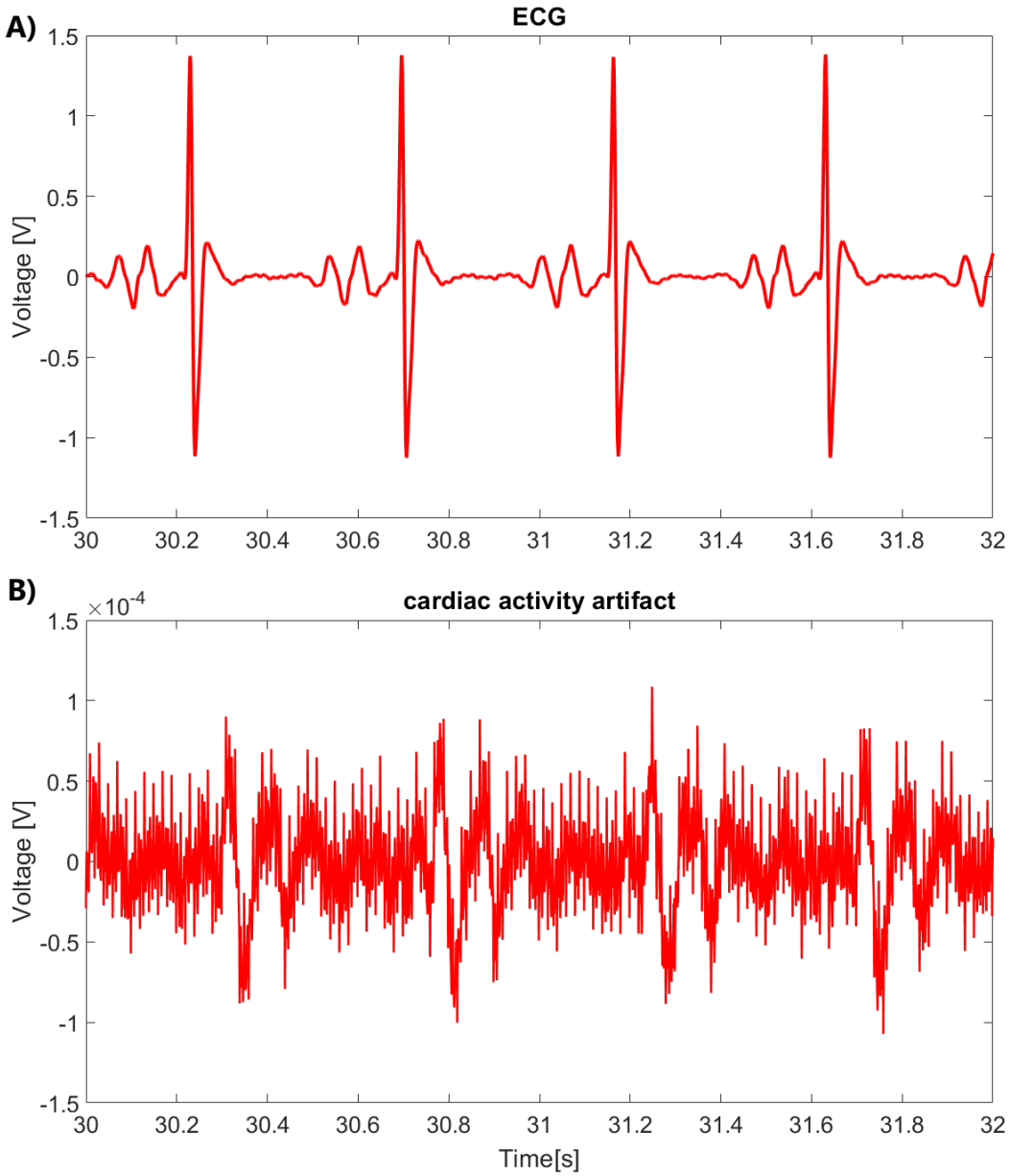

Figure 9: Comparison between ECG time course and cardiac activity related artifacts

In Figure 9 the temporal trends of a neural signal showing cardiac activity related artifacts (A) and the corresponding trend of the ECG signal (B) are shown. As can be seen, artifacts are present with a slight delay compared to the peak of the ECG signal.

- **Peak artifact**

  This artifact is characterized by a voltage value, in module, far higher than the rest of the signal. For its identification we proceeded through a simple constant

thresholding algorithm, followed by visual inspection. It has however been taken into consideration that the neural signals may contain spikes, i.e. peaks of neural activity that are of interest. Thus, the threshold level was set equal to the average of the signal ± 6 times its standard deviation.

Once the artifacts were identified, the intervals in which the signal exceeded the threshold were removed.

In Figure 10, below, an example of peak artifacts is shown. The high voltage value that characterizes them makes their identification simple.

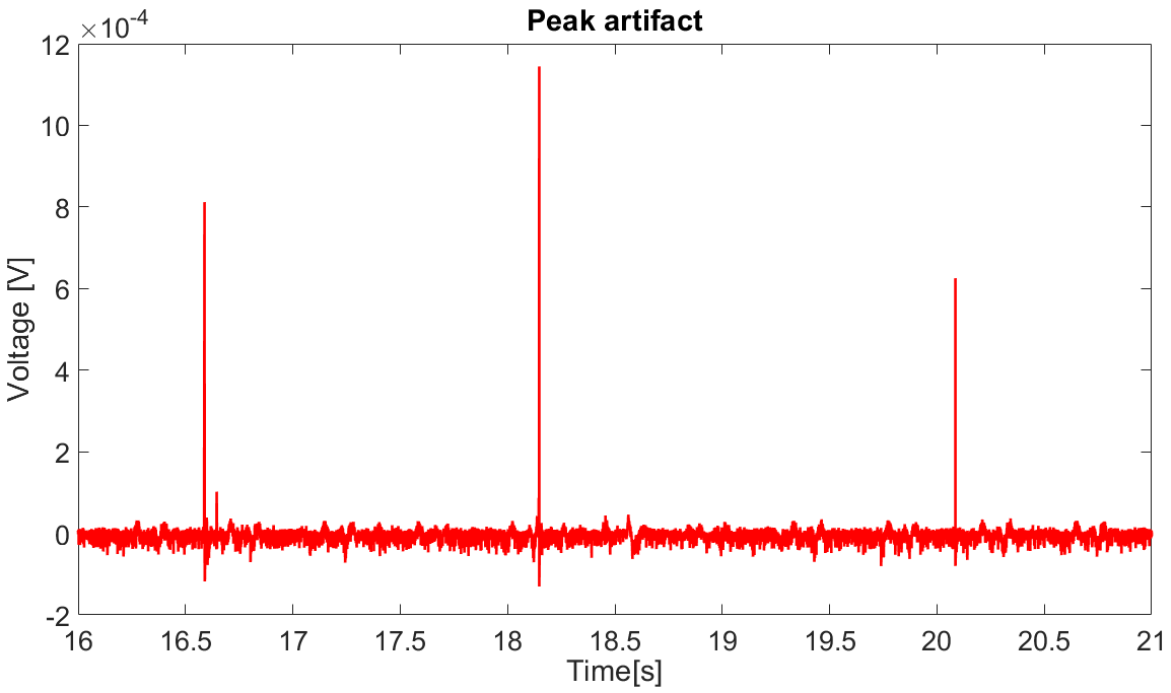

Figure 10: Example of peak artifacts

After the elimination of the artifacts, we proceeded with the filtering of the neural signals using a band-pass Butterworth filter of eight order with inferior cut-off frequency of 5 Hz and superior cut-off frequency of 5 KHz.

During the experiments, that was carried out both with SELINE and cuff electrodes, there was the possibility that the active sites were not in full contact with respectively the fascicle of the nerve or with the epineurium. This could bring to differences in the magnitude of the recorded signals. To treat this problem we decided to use an algorithm

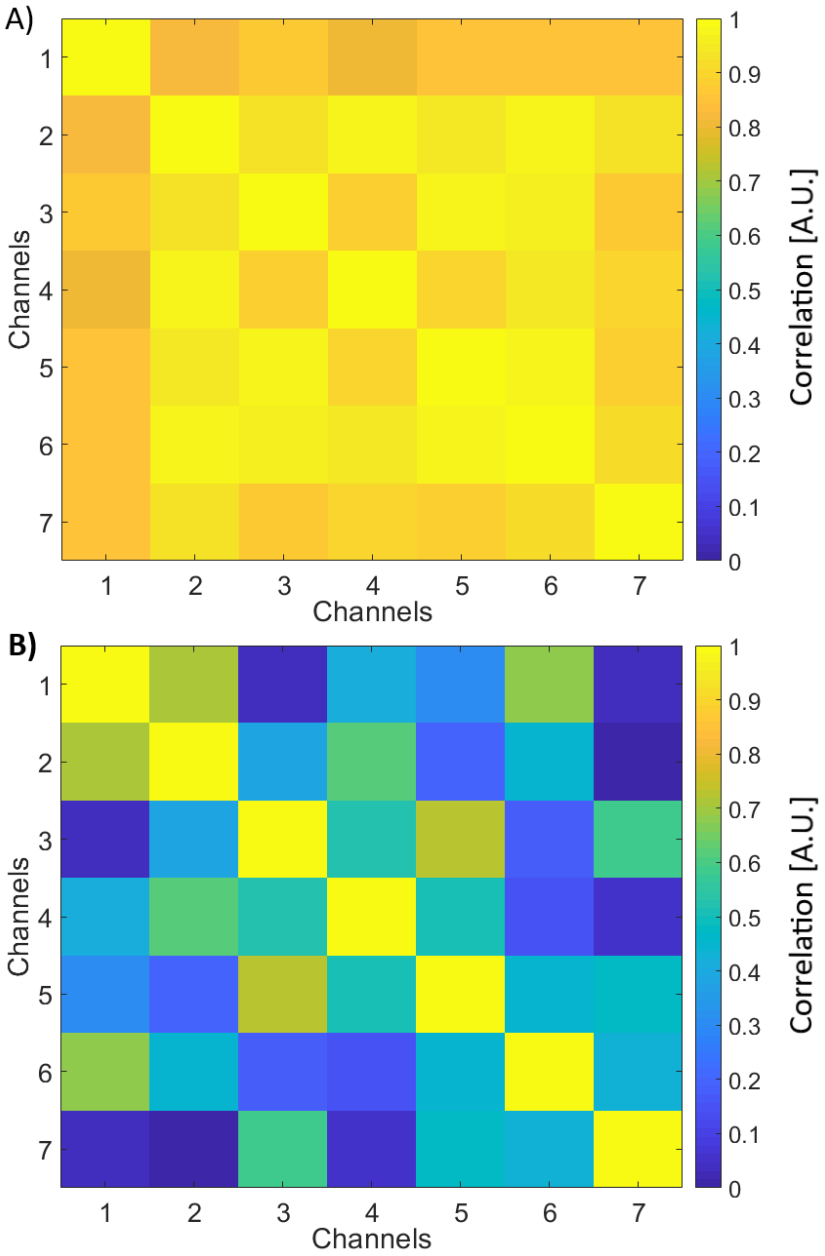

Figure 11: Correlation matrix of raw (A) and cleared (B) signal

of z-score on the channels. This algorithm, implemented by the command line zscore in Matlab, involves subtracting the signal's average and dividing it by its standard deviation.

For a signal X with mean μ and standard deviation σ, the z-score of a value x is:

$$z = \frac{(x - \mu)}{\sigma}$$

This allowed us to standardize all the channels.

Another problem that needed to be solved during data analysis was the high level of correlation between channels. After the elimination of the artifacts and the

standardization of the data, the correlation coefficients were recalculated. In this way we were able to verify whether the signal processing changed the level of correlation between the channels. Correlation coefficients again indicated a high level of correlation between channels. For this reason it was decided to proceed with the elimination of their common component. The mean component of the signals recorded from the channels was then take as reference and was subtracted to each channel [30]. The same procedure was used by S. C. M. A. Ordelman et al. to verify the presence of a neural signal component that was not visible using cuff electrodes in tripolar configuration [17] [18].

The exposed methods were applied both to the data coming from the experiments in which the SELINE electrode was used and to the data coming from the experiments in which the cuff electrode was used. In these experiments the number of active sites for the electrodes was respectively N = 10/16 for SELINE and N = 3 for cuff.

Figure 11 shows an example of the correlation coefficients before and after the common mode rejection for a baseline file. It can be clearly seen that the correlation between all the channels in the raw data (A) was very high (greater than 0.8), while, in the cleared data (B) there is correlation only between some channels. For example, between channel one and channel two or between channel three and channel five. The diagonal of the matrix is always equal to 1 since each channel is always directly correlated with itself. For the example above, correlation coefficients assume values in the range 0.8-0.98 for (A) and 0-0.73 for (B), without considering the values on the diagonal. The two range does not intersect each other. A paired t-test across channels pairs confirm that the correlation level was effectively decreased ($p<0.05$).

To conclude, any possible residual artifact was manually removed and was performed an extraction of the power spectral density of the signals. These PSDs were then evaluated in order to find the changes in the low frequency spectrum and verify if these changes were significant or not. Figure 12 show a comparison between a raw baseline signal and the same signal after processing.

The estimation of the power spectral density was made with the Welch method, described in 2.2.1. The length of the segments after the previous steps varied between 10 and 15 seconds. In order to obtain an appropriate estimation of power spectral density, the Welch method was applied using a 1 second hamming window with 50% overlap. This

allowed us to obtain an adequate estimation of the PSD because the estimation was calculated as the mean of more than ten modified spectrogram.

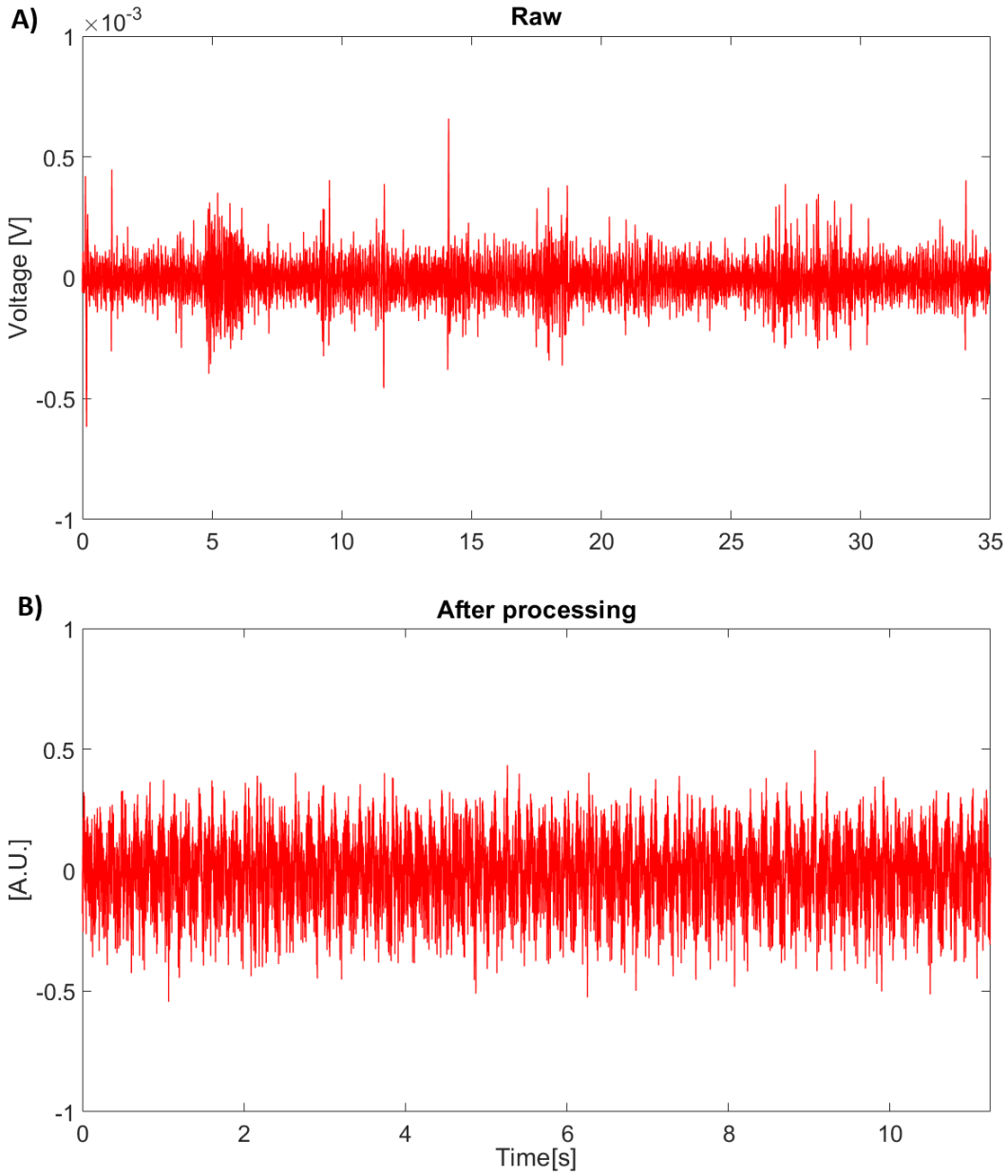

Figure 12: Comparison between raw and processed signal

The power spectral density was then evaluated in order to verify if there were significant changes in the low frequency spectrum. The evaluation was carried out considering two status of the animal, a challenge status and the baseline status that precedes the challenge. A first visual inspection shows that there were changes in the frequency between 5 and 40 Hz for the challenges of AII infusion, TV increase and RR increase. No file regarding the challenges of Sodium Nitroprussiate infusion, Glucose infusion or Insulin

injection was analyzed, so we are not able to tell if these changes were present even during these challenges.

Through the following criterion it was finally verified if a pair of PSDs, baseline-challenge, showed significant variations.

A pair of power spectral densities, estimated from the same site active in a challenge file and its previous baseline file, show a significant variation, if one of the following two inequalities is satisfied in at least two different frequency values.

$$P_{ic} - P_{ib} > mean(P_b) + 3 * std(P_b)$$

$$P_{ic} - P_{ib} < mean(P_b) - 3 * std(P_b)$$

Where the index c and b respectively stand for challenge and baseline, while the index i stand for the ith frequency.

If, for example, at frequencies f1 and f2 the first inequality is verified, then, the PSDs are considered to have significant variations.

Conversely, if at frequency f1 the first inequality is verified and at frequency f2 the second inequality is verified, the PSDs are not considered to have significant variations.

4 Results

4.1 Data analysis

The results were obtained only on a subset of the entire set of data following the method exposed in the previous paragraph. Here we discuss exclusively to the challenges regarding the BP increase caused by AII infusions, increase of the TV and RR. The results are subdivided by the challenge and by the type of electrode that was used in the experiments. This allows for a comparison between the response to the challenges and a further comparison between the different selectivity of our electrodes, i.e. Cuff vs. SELINE.

Spectral analysis allowed us to understand if the changes in the physiological status were reflected in the oscillatory activities of the neural signals. Specifically, we decided to analyze the low frequency range from 5 to 40 Hz.

In the last part of the analysis, using the criterion described at the end of 3.2, was examined whether the changes in the frequency range between 5 and 40 Hz of the PSD were significant or not. We were able to quantify, for each analyzed challenge, which channels and frequencies were modulated by the different challenge.

ANGIOTENSIN INFUSION CHALLENGE: physiological modification

The amount of AII infused to the animals during the experiments varied from 18 to 82 ml/h (see section 2.1.3.2). The baseline parameters for HR and BP values, could vary considerably between the different animals, as well as the time needed to reach the plateau. During this challenge the animals undergone a considerable increase in the values of HR and MAP, on average by 21% for the HR and 32% for MAP, with a minimum of respectively 8% and 6%.

Figure 13 shows an example of variation of the parameters BP and HR during a challenge of infusion of Angiotensin II, compared with the previous baseline.

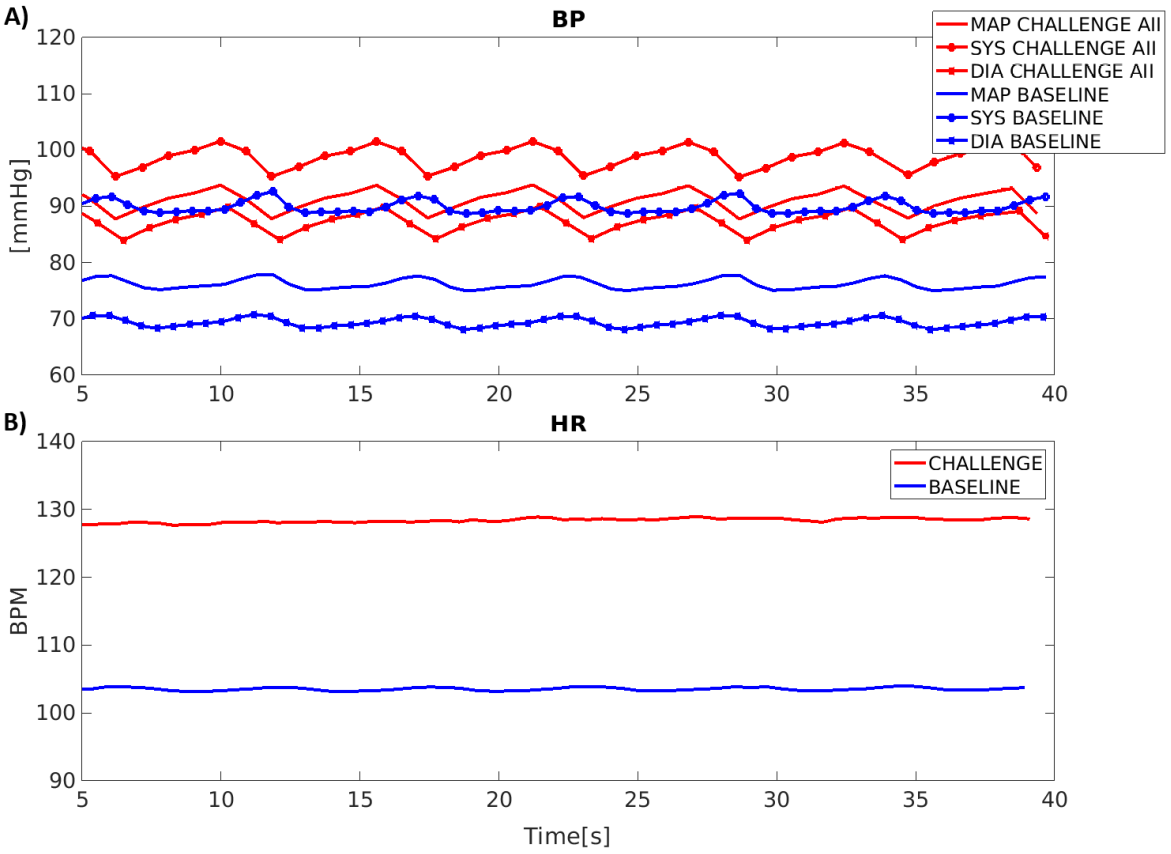

Figure 13: Comparison of the BP and HR level between a challenge of infusion of AII and the previous baseline

– **SELINE: neural modifications induced by AII**

We analyzed the PSD of three of the nine animals subjected to AII challenges. As is showed by the representative image below (Figure 14, one animal) the power spectral density of the cleared signals (see section 3.2), recorded from SELINE electrodes, are subject to visible variations in the considered frequency range. In particular, three principal changes can be seen. An increase in the power near 12 Hz and 20 Hz and a decrease near 14 Hz (see Figure 16, Figure 17 and the text below for the statistical quantification). These variations are not visible in all channels and this could be an indicator that SELINE electrodes can record selectively from the nerve.

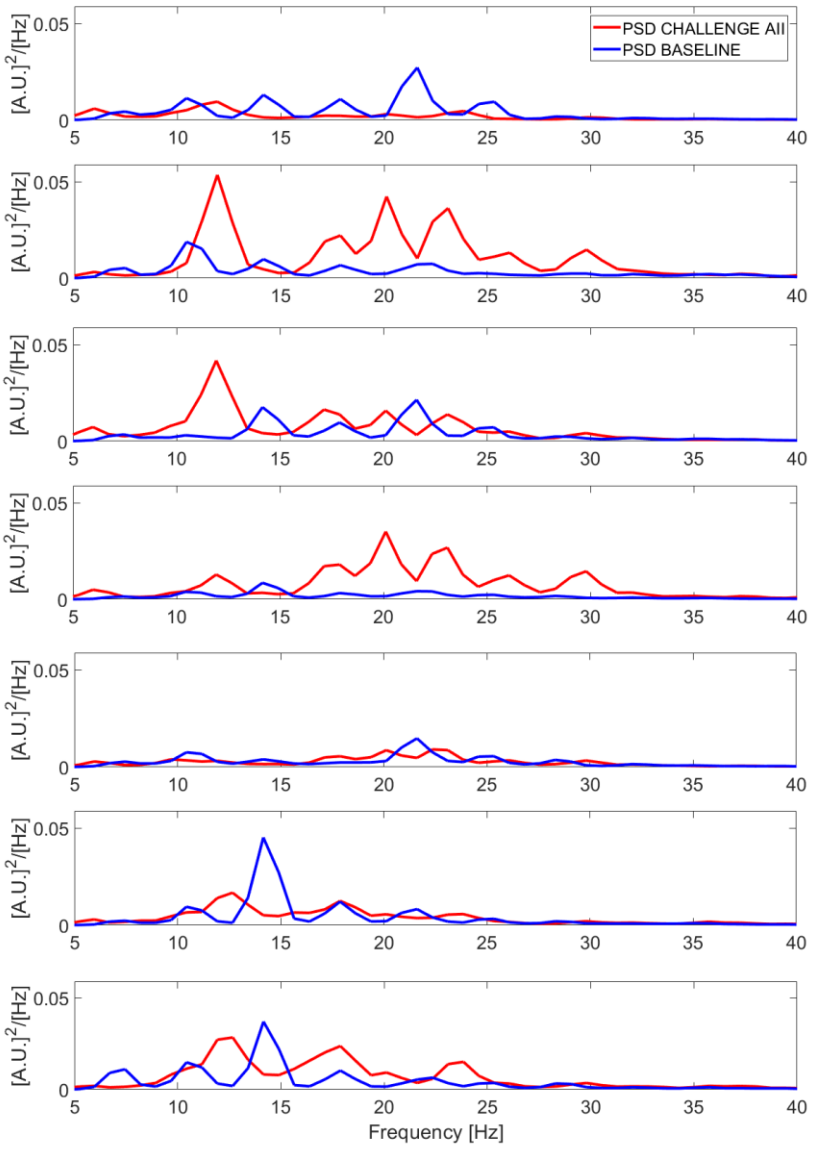

Figure 14: PSD of the processed signal of a challenge of AII and the previous baseline recorded with SELINE electrode

– **CUFF: neural modifications induced by AII**

Even here, as it can be seen in the following image (Figure 15, one animal), the power spectral density of the signal recorded with cuff electrodes show visible variations between the baseline and challenge status. However, it as to be seen that these variations affect a wider range of frequency (from 7 to 25 Hz) with respect to the one of SELINE previously shown (see Figure 16, Figure 17 and the text below for quantification). Another important observation is that the changes are present in each channel, this could imply that cuff electrodes could not allow for a selectivity recording.

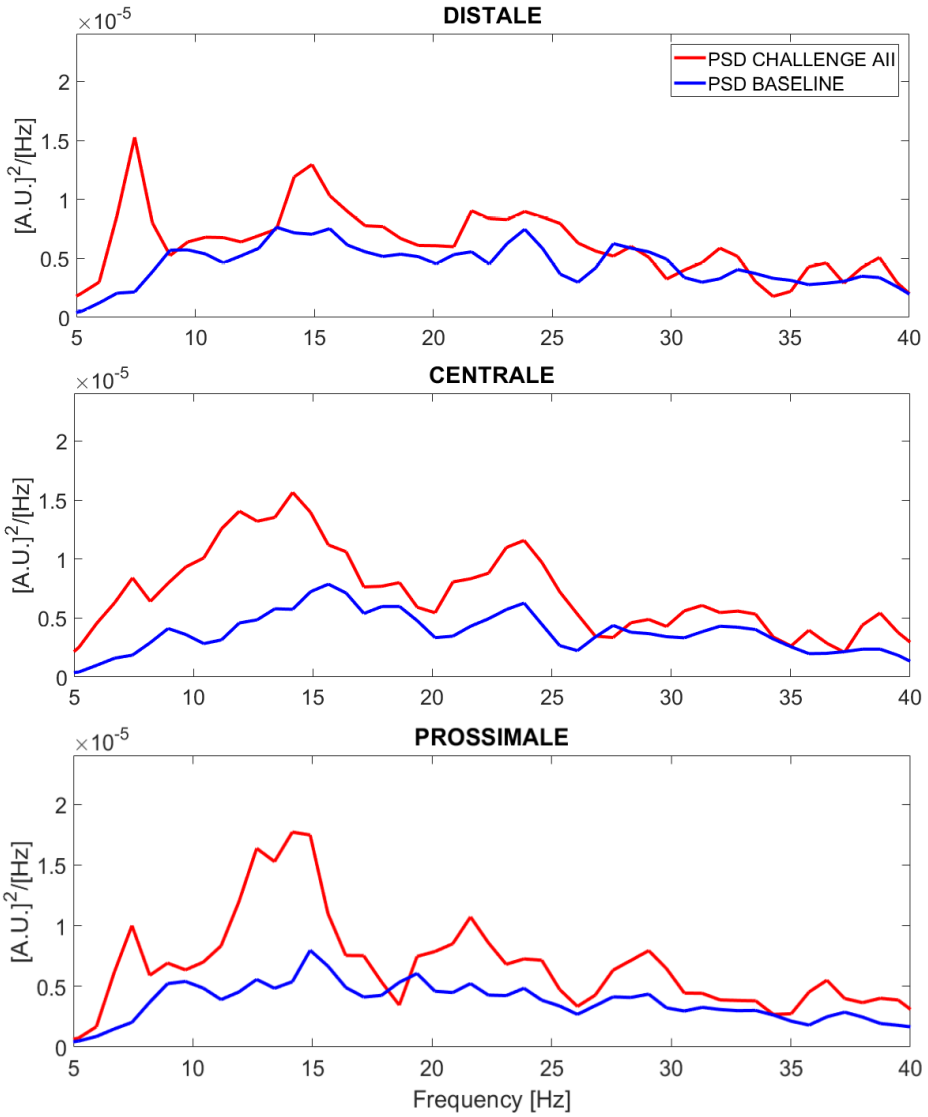

Figure 15: PSD of the processed signal of a challenge of AII and the previous baseline recorded with CUFF electrode

To test whether these modulations were significant, we implemented the statistical test reported at the end of section 3.2. Figure 16 report the frequencies in which a significant modulation was found. Channels in which only one frequency report a significant modulation were not considered. Panel (A), (B), and (C) refer to experiment in which SELINE electrodes were used, while panel (D) refer to an experiment with CUFF electrode. In the latter, because of the wider range of frequency affected by the modulations, only few frequencies result to have a significant modulation. Furthermore, with the use of an unpaired t-test ($p<0.05$) we verify that the modulation observed with CUFF electrode (increase: 1.03e-05 ± 1.05e-06, decrease: -1.18e-06 ± 4.25e-07) were significantly lower than the one observed with SELINE (increase: 0.01 ± 0.012, decrease: -0.01 ± 0.01).

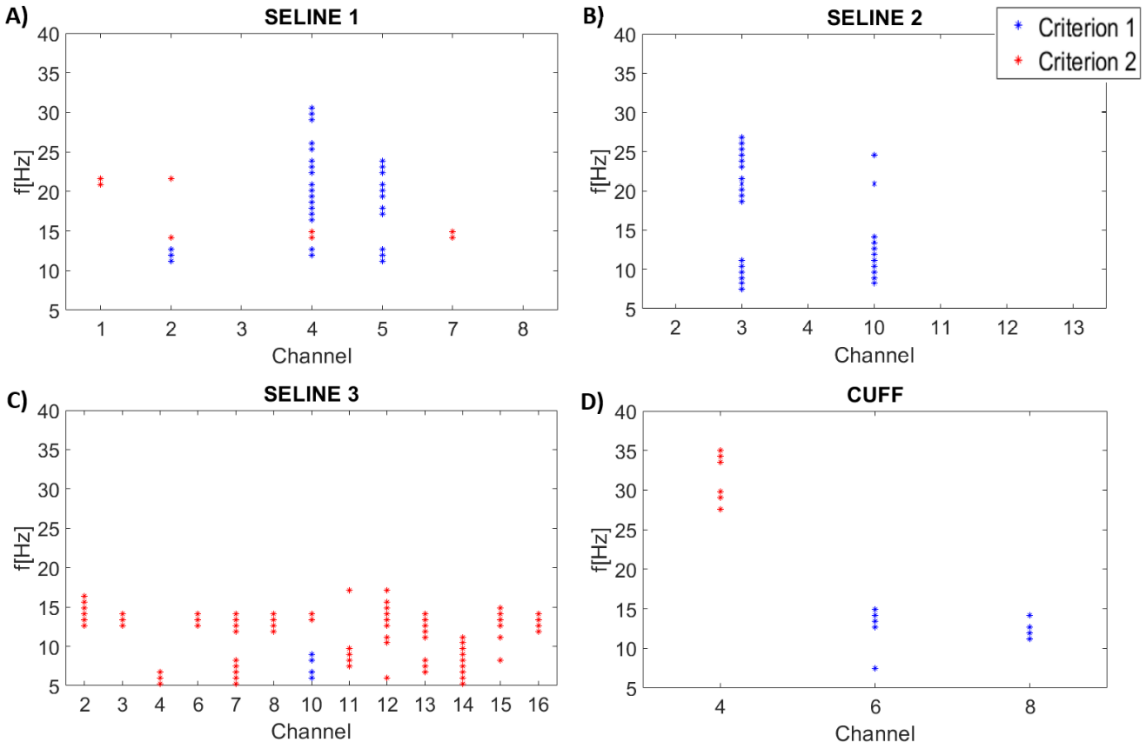

Figure 16: Modulated frequency for each channel during challenges of infusion of AII in different experiments. Title reports the electrode type used in each experiment.

Figure 17 shows the percentage of modulated channels during the different experiments of AII infusion. The first three value are relative to challenges in which the animals were implanted with SELINE electrodes, while the last value is relative to an experiment performed with cuff electrode. It's important to notice that the percentage of modulated channels with SELINE implant can vary (66.67 % ± 35.95). This may mean that the used electrodes can provide selectivity during recording. For cuff electrode, instead, all the channels were subject to modulation, but results on an individual animal are not enough to draw conclusions. The modulation of all channels may be due to the structure of the electrodes.

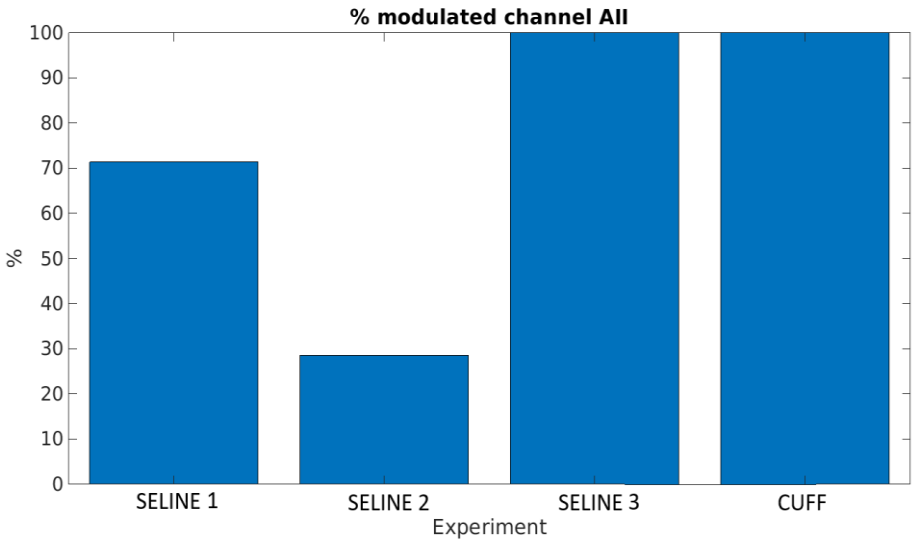

Figure 17: Percentage of modulated channels during challenges of infusion of AII in different experiments

TV CHALLENGE: physiological modifications

Challenges of TV increment were performed by imposing very precise variations ranging from 25% to 100%, of baseline TV. Also in this case variability among the absolute value of baseline TV in the experiments is present (see Table 3). Baseline level was modified during the different experiments from a starting value of 400cc to 450cc.

In Figure 18 an example of the effect of TV increment in the respiratory cycle is shown. During this challenge a doubling of the respiratory volume was imposed, from 450cc to 900cc.

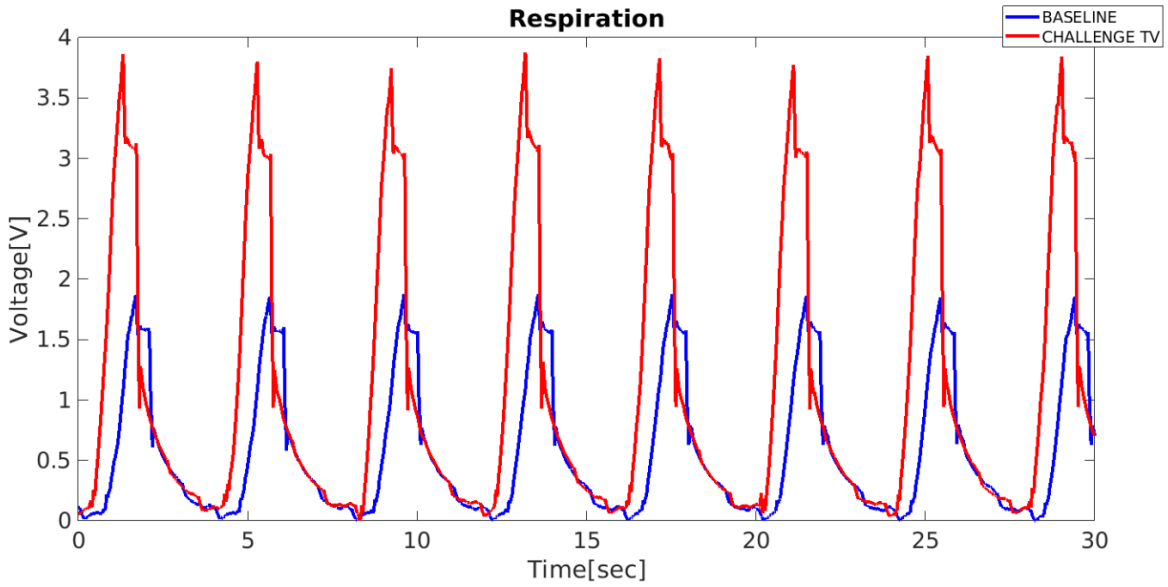

Figure 18: Comparison of the respiratory activity during a challenge of increase of TV and the previous baseline

– **SELINE: neural modifications induced by TV**

Pigs in which the recording was done with the use of SELINE electrodes showed variation in the interested range of frequency of the power spectrum, see the image below (Figure 19, one representative animal). An increase in power around 13 Hz can be noted (see Figure 21, Figure 22 and the text below for quantification). Again, the presence of these variations in a subset of channels could be considered as an indicator of the possibility that SELINE electrodes provide selectivity during recording.

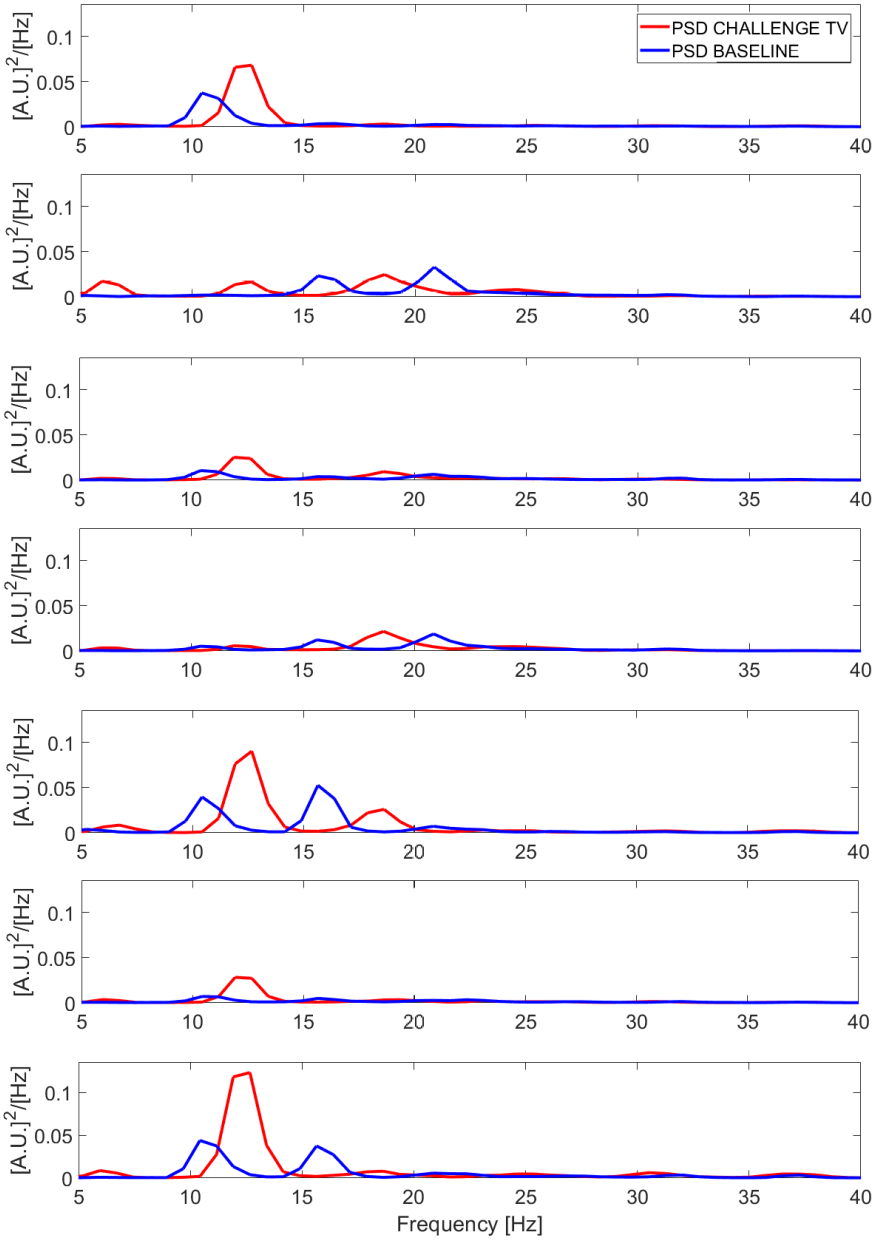

Figure 19: PSD of the processed signal of a challenge of increase of TV and the previous baseline recorded with SELINE electrode

– **CUFF: neural modifications induced by TV**

The results obtained from the data recorded by CUFF electrode show variations in all the channels. Similarly to the challenge of AII infusion, the variations of the power spectrum affect a wider range of frequency (see Figure 20) in respect to the results obtain with the use of SELINE, more or less all the interested range 5-40 Hz (see Figure 21, Figure 22 and the text below for quantification).

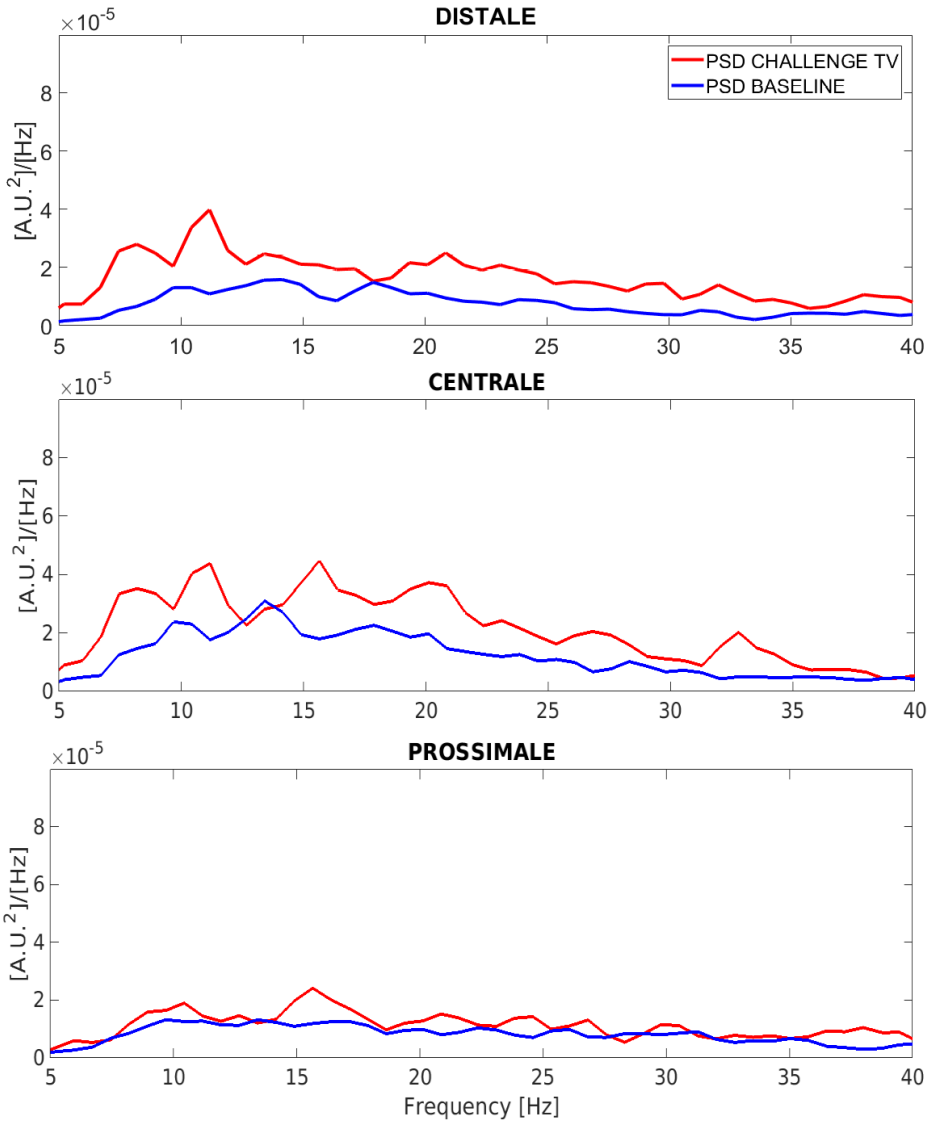

Figure 20: PSD of the processed signal of a challenge of increase of TV and the previous baseline recorded with cuff electrode

Figure 21 shows for each channel of different experiment the frequencies in which a significant modulation was found (we used the statistical test reported at the end of section 3.2). The panels (A), (B) and (C) refer to experiment with SELINE electrodes, while panel (D) refer to an experiment with CUFF electrode. Even in this case, because of the wider range of frequency affected by the modulations during CUFF recording (Figure 20, one representative animal), only few frequencies result to have a significant modulation. Again, with the use of an unpaired t-test ($p<0.05$) we verify that the modulation observed with CUFF electrode (increase: 2.28e-05 ± 4.1e-06, decrease: -1.86e-06 ± 9.9e-07) were significantly lower than the one observed with SELINE (increase: 0.035 ± 0.027, decrease: -0.021 ± 0.016).

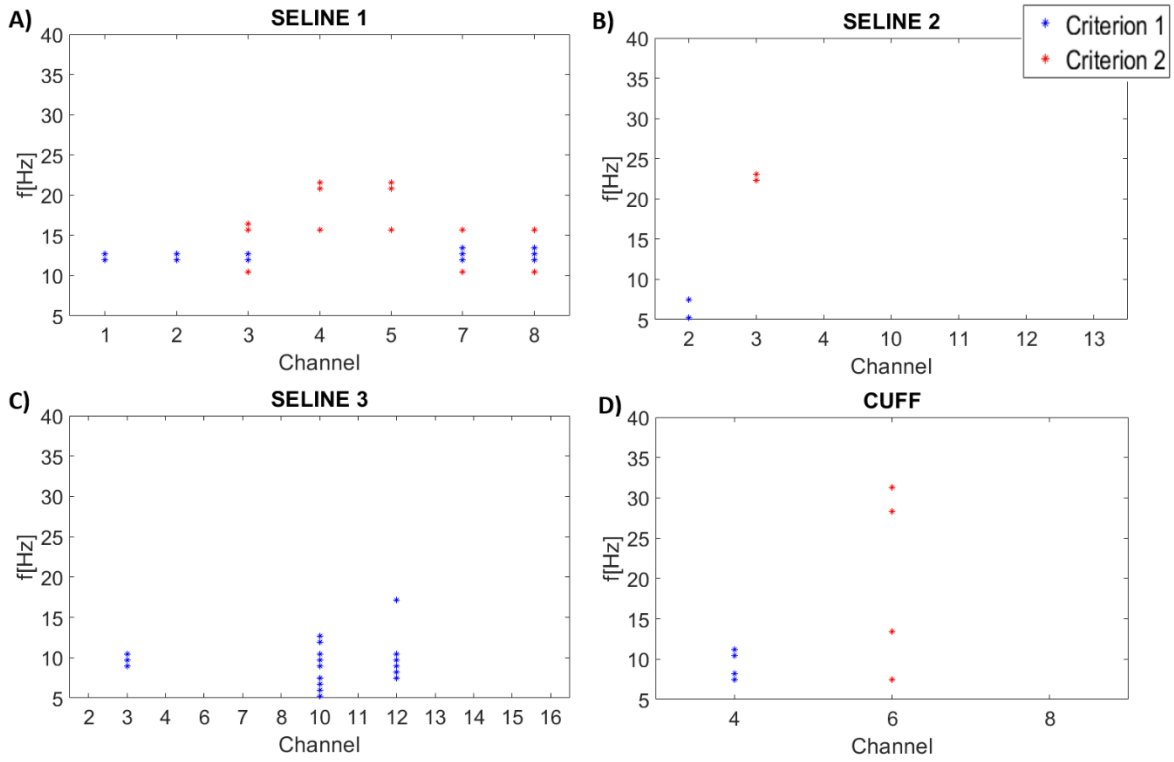

Figure 21: Modulated frequency for each channel during increase of the respiratory volume in different experiments- Title reports the electrode type used in each experiment.

In Figure 22 the percentage of modulated channels for three experiments with SELINE implant and one with cuff implant are shown. The percentage of modulated channels in the experiments with SELINE implant can vary (50.55 % ± 42.91). This, as before, may mean that this type of electrode offers the possibility to selectively record from the fascicles. The difference in the percentage of modulated channels may be due to different orientation of the insertion of the electrodes. It has to be noticed that the experiment with cuff implant reports modulations in 66% of the channels. This may mean that selective recordings can also be performed with cuff electrodes, but these considerations are limited because of the low number of active sites of the CUFF electrode used in this experiment and further analysis should be made to confirm this preliminary result.

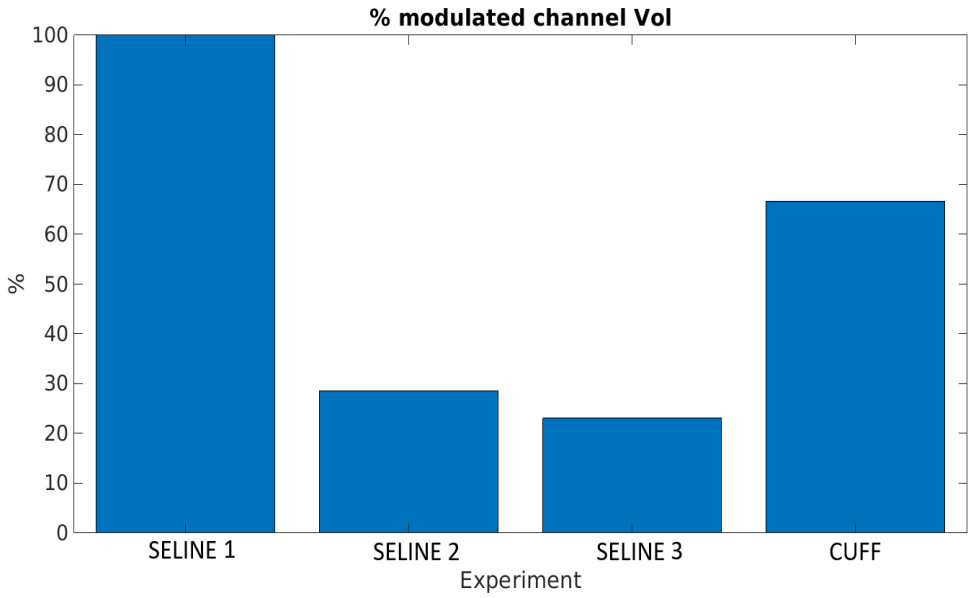

Figure 22: Percentage of modulated channels during increase of the respiratory volume in different experiments

RR CHALLENGE: physiological and neural modifications

The challenges of increment of the respiratory rate was carried out, as for the challenges of TV increment with the use of Servo Ventilator 900c. During these challenges an increment of 50-100% of the respiratory rate was imposed. It was noticed that during these challenges an undesirable effect take place. In fact, as is shown in Figure 23, the increase of the respiratory rate brings a reduction of the tidal volume, 20-50%, depending on the imposed change of RR. However, this challenge differs from the previous one due to the main effect of the RR increment, so it can be analyzed as a challenge where both effects are present.

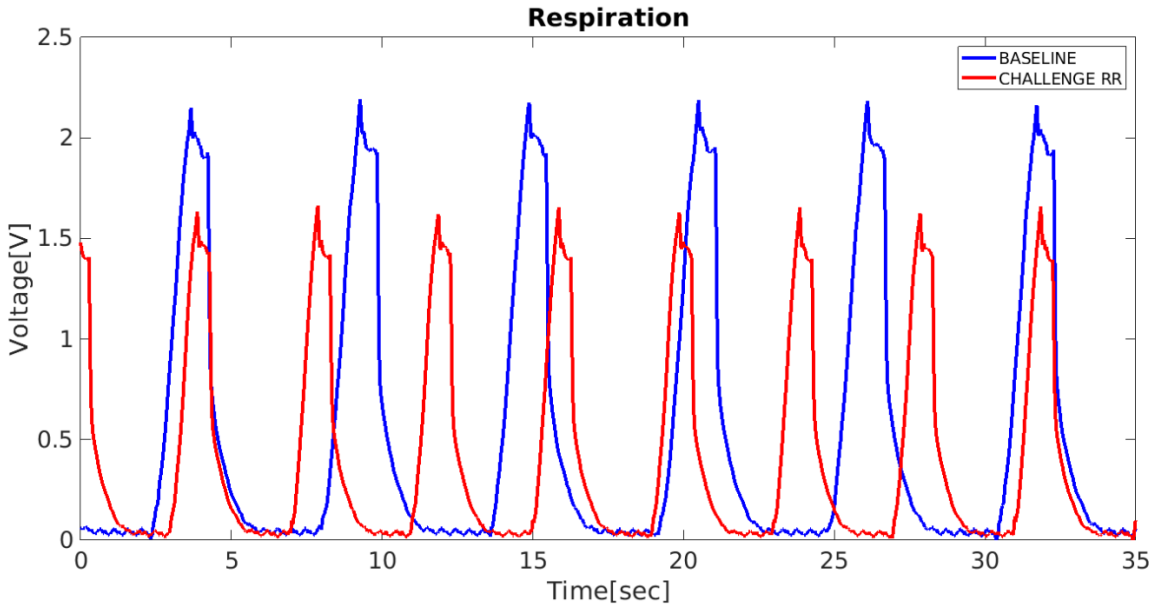

Figure 23: Comparison of the respiratory activity during a challenge of increase of RR and the previous baseline

For this challenge the results are relative only to data recorded through the use of SELINE electrodes. This because at the end of the pre-processing (Section 3.1) no data coming from cuff acquisition showed significative variation in the PSD of the neural activity. However, PSDs of the neural signals coming from SELINE recordings (see Figure 24) show significant variation in the range of frequency from 5 to 40 Hz (see Figure 25 and Figure 26). Unlike the previous challenges, the variations here affect all channels. But as before, these are relative to a narrow range of frequencies, around 12 Hz (Figure 24, one animal).

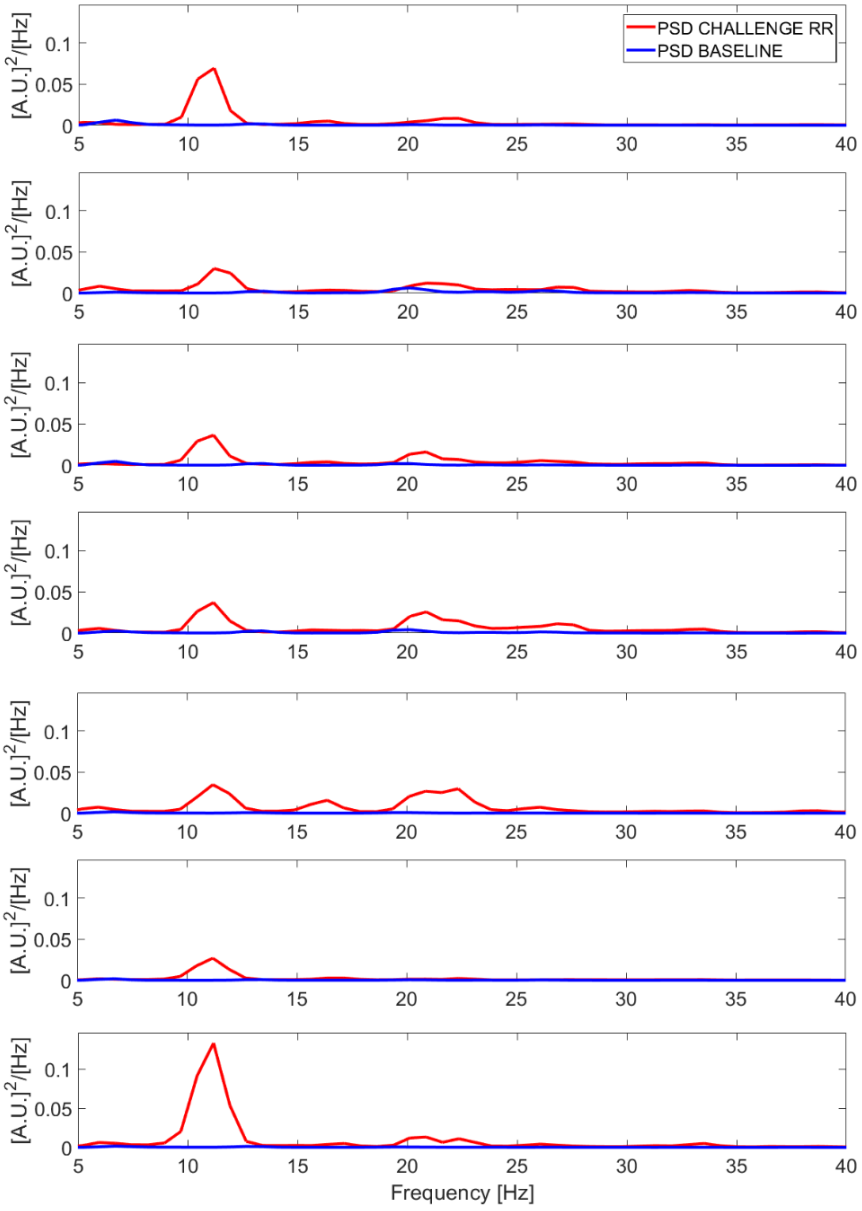

Figure 24: PSD of the processed signal of a challenge of increase of RR and the previous baseline recorded with SELINE electrode

As previously stated, for the challenge of increment of the respiratory rate there are no results relative to cuff implant because we were not able to identify modulation in these recordings. Figure 25 shows for each channel of different experiment the frequencies in which a significant modulation was found. In the first and last panel (A and C, respectively) we can observe that the significant modulation, caused by the challenge, have a common range in which are present ,10-15 Hz.

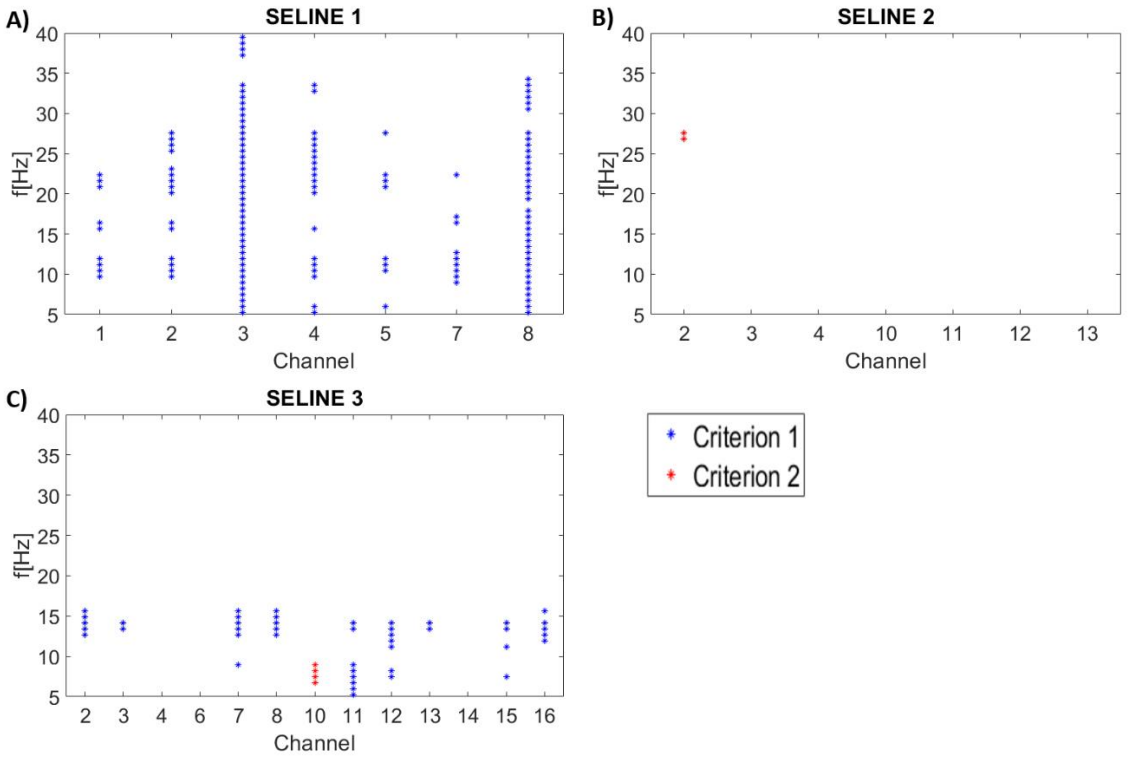

Figure 25: Modulated frequency for each channel during increase of the respiratory volume in different experiments. Title reports the electrode type used in each experiment.

In Figure 26 are shown the percentage of modulated channels for experiments with SELINE electrodes. As in previous challenges, percentages vary in experiments (63.74 % ± 44.35). So, as before, this result may involve the possibility of selective recording with these electrodes.

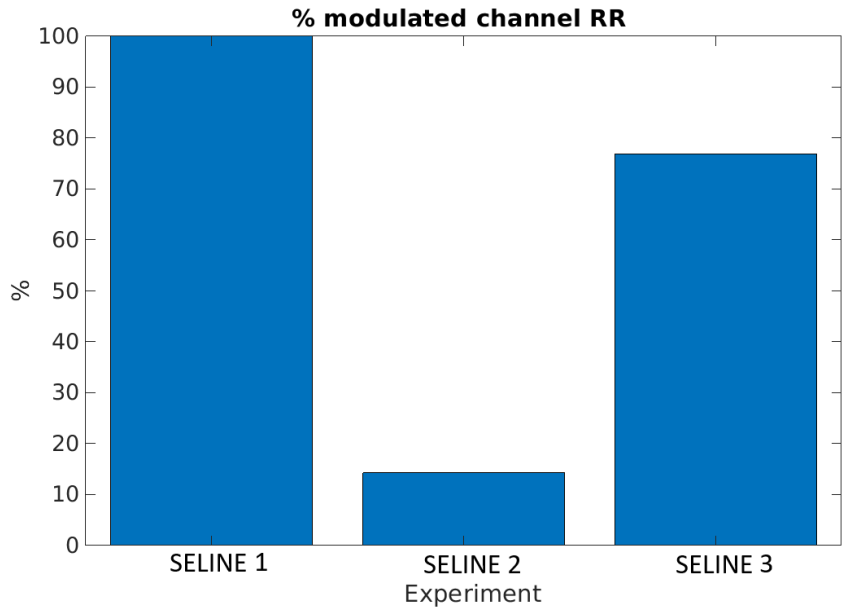

Figure 26: Percentage of modulated channels during increase of the respiratory rate in different experiments

4.2 Histology

To check the correctness of the electrode implantation, the cervical vagus nerve was separate from the rest of the body by a length of 7-10 cm. These segments, on which the electrodes were implanted, were taken at the end of the experiments and subjected to a histological analysis. The analysis was performed following a classical preparation in hematoxylin and eosin. This type of preparation is a standard method used both for the identification of tissue structures [31] [32] [33] and for diagnostics [34]. The procedure was carried out following these steps:

- Fixation of the nerve with the implanted electrode in paraformaldehyde 4% for 20 hours
- sequential passages of dehydration in alcohol 70-80-90-99%
- clarification with xylol and embedding in paraffin
- cutting at the microtome of 10 μm thick slices for the length of the implant plus one centimeter before and one centimeter after
- staining with hematoxylin and eosin

The resulting slices were then visualized with an optical microscope. Finally, with the use of the software Rhinoceros 6, a three-dimensional nerve reconstruction was achieved.

Figure 27 shows an example of histological images obtained after staining with hematoxylin and eosin.

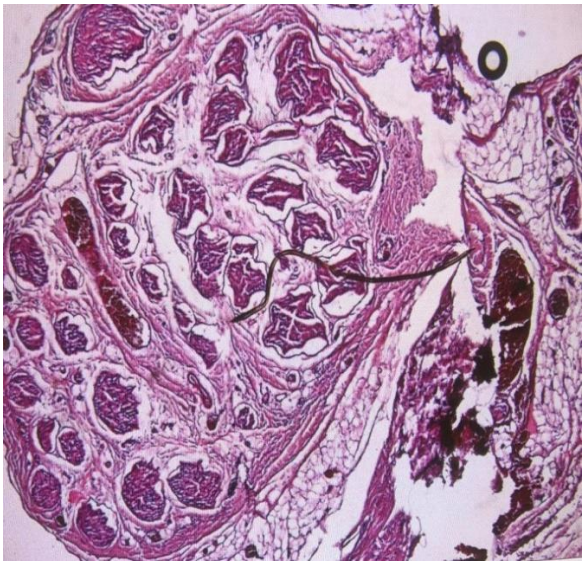

Figure 27:Histology of vagus nerve with implanted SELINE

The 3D reconstruction of the nerve allows us to visualize the distribution of the fascicles in the taken segment. In addition, having maintained the implant, it is possible to check which fascicles were most in contact with the electrode. This, in future analysis, could help to identify the fascicles that transmit certain types of signals.

In Figure 28 nerve reconstruction performed with Rhinoceros 6 software can be observed. This reconstruction is related to the cervical vagus nerve with implantation of a SELINE electrode, the element highlighted in yellow. As you can see from the image, 3D nerve reconstruction also allows you to verify if the electrode used during the experiment was correctly implanted.

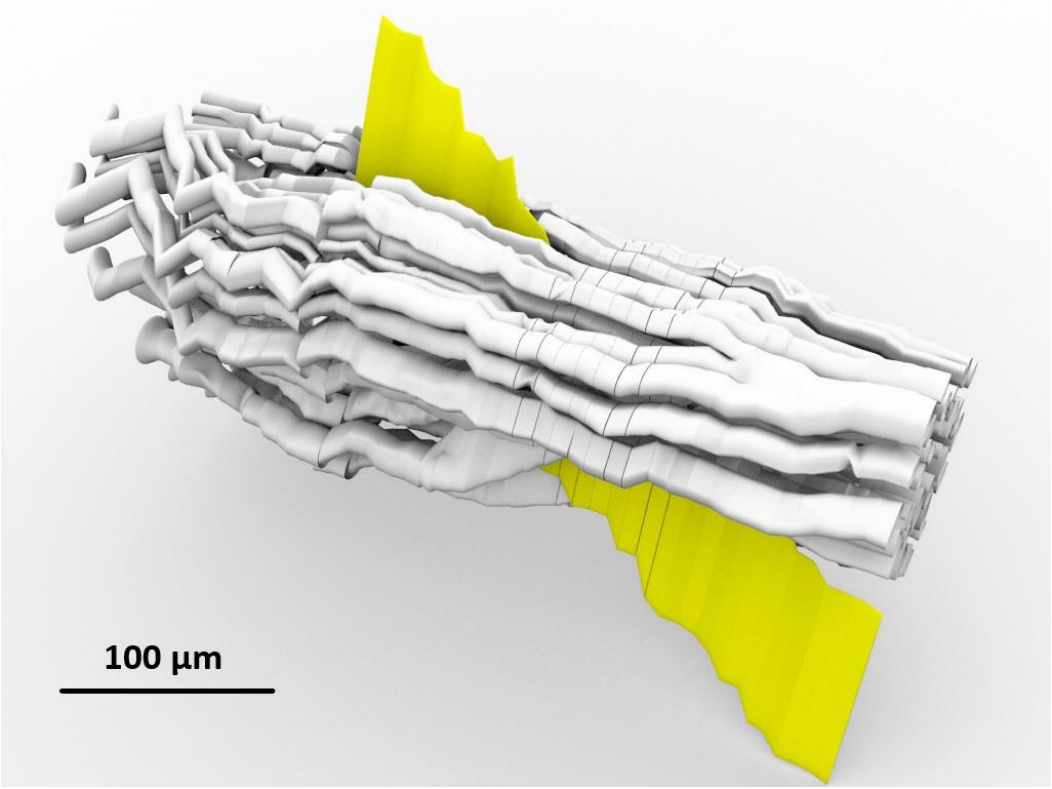

Figure 28: 3D reconstruction of a section of cervical vagus nerve

4.3-Discussion

The purpose of our analysis was to verify whether the challenges of angiotensin infusion, increased respiratory volume and increased respiratory rate, significantly modulate the neural activity of the vagus nerve. Neural signals recorded by the active sites of the electrodes had a high level of intrinsic correlation and several artifacts (as reported in section 3.2). It was therefore necessary to process these signals and remove these artifacts and their common component.

Finally, the power spectral density of the cleared signals was analyzed. This analysis allowed to visualize the modulations that have taken place during the course of the challenges and verify if they were or not significant.

It was noted that modulations occurred only in some channels in most experiments, as evidenced by the figures 17,22,26. In this regard it is therefore appropriate to consider the orientation with which the electrodes are implanted. Different orientations result in the visualization of such modulations in different channels. A second aspect to take into account is the interface between electrode and nerve. From the results shown in figures 17,22,26 it seems that the SELINE electrode (intraneural) is able to provide a greater distinction of neural activity than the cuff electrode (epineural). However, it should be noted that the results relative to implant with cuff electrode come from a single experiment and, therefore, more experiments are needed to support this hypothesis.

The statistical test allows the identification of the frequency in which the modulations for each channel were significant. The challenge of infusion of Angiotensin II show significative modulation in the range 7-30 Hz. Using SELINE electrodes we were able to identify a significative decrease at 14 Hz and two significative increase: one at 12 Hz and the other from 15 to 25 Hz. With CUFF electrode we observe an increase of the PSD in the range 7-30 Hz, with only few frequencies in which these modulations were identified as significative. For the challenge of increase of the tidal volume, we identified, with SELINE electrodes, a significative increment of the PSD at 13 Hz and a significative decrement at 16 Hz. While, with CUFF electrode, we observed an increase of the PSD in all the interested frequency range, 5-40 Hz. As for the AII challenge, because modulations occur in a wider range of frequency, we identify only few frequencies in which these were

significant. Last, for the challenge of increase of the respiratory rate, we were able to identify a significant increase in the range from 10 to 15 Hz in two over three pigs.

5 Conclusions and perspectives

During this thesis we were able to characterize the modulations in the VN associated to some physiological alterations of the respiratory and cardio-circulatory systems. Moreover, the different properties of SELINE and CUFF electrodes in capturing such modulation were compared.
With the recent development in the field of neural interfaces, the possibility of being able to decode and therefore understand the language of our body, is becoming more and more within reach. This development has led to the creation of a new field of research, the bioelectronic medicine [3] [35].
Bioelectronic medicine, and particularly Electroceutics, offer great possibilities for development in the field of treatment of diseases such as hypertension, epilepsy, diabetes and other diseases in which our nervous system is involved. Electroceutics has in fact the potential to be able, in the future, to replace the current methods of pharmacological treatment with treatments that use the electrical stimulation of the nervous system [2] [36].

In the literature it is possible to find papers in which is indicated the possibility to use this type of stimulation for the treatment of diseases [12] [13] [16] [25]. However, in many of the results obtained, reference is made to the fact that the electric stimulation may induce adverse effects.

The purpose of this thesis was to verify the presence of modulations of the neural activity of the vagus nerve induced by alterations in the physiological and metabolic state, so as to consider these modulations as candidate of neural biomarkers.

During the experiments different challenges were carried out: increment of the respiratory volume and frequency; challenges related to the cardio-circulatory system, increase and decrease in blood pressure, with consequent variation in heart rate and glycemic challenges with glucose infusion and insulin injections.

Variations in the power spectral density of neural signals between baseline status and physiological alteration status have been evaluated. As has been reported in Chapter 4, in several experiments the modulations of neural activity, in the range 5-40 Hz, were

significant. However, it remains to be seen whether these modulations can be used to obtain information on physiological status of the animals.

The choice of neural interfaces to be used to retrieve the signal is crucial. During our experiments, two types of electrodes were used: the cuff electrodes (epineural), which wrap the nerve and interface with the epineurium and the SELINE electrodes (intraneural), which are inserted into the nerve and interface with the fascicles contained therein, thus becoming more invasive. The obtained results, discussed in section 4.1, seem to show not only that there is selectivity of activation of the fascicles inside the nerve, but also that it is more easily identifiable using SELINE electrodes. However, the data given in this thesis are not sufficient to substantiate this hypothesis and further studies will be necessary in order to verify it.

Given their way of interfacing with the nerve, SELINE electrodes then introduce another factor to be taken into consideration, that is the orientation with which the implant is carried out. In section 4.1 it is shown that the percentage of channels in which significant modulations are visible can vary between the different experiments. The hypothesis is that different orientations of the insertion have led the electrodes to interface with different fascicles. In this way the recorded signals are dependent on the orientation with which the implant is carried out. Histological analysis of the nerve with the implanted electrodes, reported in section 4.2, are therefore useful not only to understand the structure of the nerve under examination, but also to understand where the recorded signals come from. Once their origin is understood, it will be possible not only to carry out implants that collect the signal only from the fascicles of interest, but also to carry out electrical stimulations that will modulate only the information we want.

The studies carried out here, although they seem to contain relevant information, have certain limitations that must be taken into account. First of all, the analyses carried out and the results obtained are related only to the range of low frequencies 5-40 Hz. It is still to be verified whether, as for the results shown by Sevcencu et al. in [11] [14] [21], the signals recorded by us contain information in high frequency (>800 Hz).

Another limitation of our analysis concerns the dynamical regimes that have been analyzed. Indeed, we have carried out the analysis by considering time intervals where the physiological signals were stationary. A further analysis will therefore have to be

carried out on the transient zones in order to verify the temporal behavior of the modulations that have been obtained here. This analysis, comparing changes in physiological state with variations in neural activity modulations, may be useful in identifying possible neural biomarkers.

Finally, the data comes from acute experiments in which the animals were kept under anesthesia and fasting from the evening before. In the future, it will be necessary to check whether the results obtained in our study could be also valid in long-term experiments. This should allow us to verify whether the specific types of implanted electrodes are usable for a long period of time without adverse effects. It will also allow to verify if the reported information is obtainable in normal conditions, that is with the pigs free to move and eat. Since the vagus nerve innervate both the intestine and the stomach, this last point is also useful for obtaining data on digestive activity [46].

To conclude it is necessary to say that other algorithms for data analysis, such as ICA or wavelet decomposition [42] [43], can be used to improve the results. In addition, it will be necessary to implement the code in such a way that the signals can be processed in real time. This will allow to develop close-loop stimulation therapies in which information on the physiological state will be extracted from recorded signals and, if necessary, the treatment of electrical stimulation will be performed [44] [45].

6 BIBLIOGRAPHY

1. *The revolutionary future of bioelectronic medicine.* **Tracey, Kevin J.** 2014, Bioelectron. Med., Vol. 1, p. 1.

2. *A jump start for electroceuticals.* **Famm, K. et al.** 2013, Nature, Vol. 496, pp. 159–161.

3. *Bioelectronic medicines: a research roadmap.* **Karen Birmingham, Viviana Gradinaru, Polina Anikeeva, Warren M. Grill, Victor Pikov, Bryan McLaughlin, Pankaj Pasricha, Douglas Weber, Kip Ludwig & Kristoffer Famm,.** 2014, Nature Reviews Drug Discovery, Vol. 13, pp. 399–400.

4. **R. M. Berne, B. M. Koeppen, and B. A. Stanton.** *Berne & Levy physiology.* 6. Philadelphia : Mosby/Elsevier, 2010.

5. **Kenneth W. Horch, Gurpreet S. Dhillon.** *Neuroprosthetics theory and practice (series on bioengineering biomedical engineering).* s.l. : world scientific, 2004. Vol. 2.

6. **Jean-Pierre Barral, Alain Croibier.** *Manual Therapy for the Cranial Nerves.* 2009.

7. **Squire, L. R.** *Fundamental neuroscience.* 4. Amsterdam; Boston : Elsevier/Academic Press, 2013.

8. *The inflammatory reflex.* **Tracey, Kevin J.** 2002, Nature, Vol. 420, pp. 853-859.

9. *Effect of selective vagal nerve stimulation on blood pressure, heart rate and respiratory rate in rats under metoprolol medication.* **Gierthmuehlen M, Plachta D. TT.** 2016, Hypertens Res, Vol. 39, pp. 79–87.

10. *Vagus Nerve as Modulator of the Brain–Gut Axis in Psychiatric and Inflammatory Disorders.* **Breit S, Kupferberg A, Rogler G and Hasler G.** 2018, Front. Psychiatry, Vol. 9.

11. *Prospective Long-Term Study of Vagus Nerve Stimulation forthe Treatment of Refractory Seizures.* **C. M. DeGiorgio, et al.** 9, 2000, Epilepsia, Vol. 41, pp. 1195-1200.

12. *VNS in drug resistant epilepsy: preliminary report on a small group of patients.* **Franzoni, et al.** 30, 2010, Italian Journal of Pediatrics, Vol. 36.

13. *A neural blood pressure marker for bioelectronic medicines for treatment of Hypertension.* **Cristian Sevcencu, Thomas N. Nielsen, Johannes J. Struijk,.** 2017, Biosensors and Bioelectronics, Vol. 98, pp. 1–6.

14. *A Respiratory Marker Derived From Left Vagus Nerve Signals Recorded With Implantable Cuff Electrodes.* **Sevcencu C., Nielsen T.N., Kjærgaard B., Struijk J.J.** 2017, Neuromodulation.

15. *Blood pressure control with selective vagal nerve stimulation and minimal side effects.* **Plachta D. T., Gierthmuehlen M., Cota O et al.** 2014, J Neural Eng.

16. *Vagus nerve stimulation inhibits cytokine production and attenuates disease severity in rheumatoid arthritis.* **Koopman, F.A., Chavan, S. S., Miljko, S., Grazio, S., Sokolovic, S., Schuurman, P. R., Mehta, A. D., Levine, Y. A., Faltys, M., Zitnik, R., Tracey, K. J., Tak P. P.** 29, 2016, Proceedings of the National Academy of Sciences, Vol. 113, pp. 8284-8289.

17. *Average reference recording from the vagal nerve reveals an evoked indirect response.* **Ordelman S C M A, Kornet L, Cornelussen R, Buschman H P J and Veltink P H.** 2009, Conf. on Neural Engineering.

18. *An indirect component in the evoked compound action potential of the vagal nerve.* **Simone C M A Ordelman, Lilian Kornet, Richard Cornelussen, Hendrik P J Buschman and Peter H Veltink.** 2010, J. Neural Eng., Vol. 7.

19. *Single-fiber recordings of unmyelinated afferents in pig.* **Otilia Obreja, Martin Schmelz.** 2010, Neuroscience Letters, Vol. 470, pp. 175–179.

20. *An Intraneural Electrode for Bioelectronic Medicines for Treatment of Hypertension.* **Sevcencu C., Nielsen T.N., Struijk J.J.** 2018, Neuromodulation.

21. *First demonstration of velocity selective recording from the pig vagus using a nerve cuff shows respiration afferents.* **B. W. Metcalfe, T. N. Nielsen, N. de N. Donaldson, A. J. Hunter, J. T. Taylor.** 2017, Biomedical Engineering Letters.

22. *Structural versus functional modulation of the arterial baroreflex.* **Chapleau MW, Cunningham JT, Sullivan MJ, Wachtel RE, Abboud FM.** 1995, Hypertension, Vol. 26, pp. 341–347.

23. *Recording and Decoding of Vagal Neural Signals Related to Changes in Physiological Parameters and Biomarkers of Disease.* **Zanos, T. P.** 2019, Cold Spring Harb Perspect Med.

24. *Identification of cytokine-specific sensory neural signals by decoding murine vagus nerve activity.* **Zanos TP, Silverman HA, Levy T, Tsaava T, Battinelli E, Lorraine PW, Ashe JM, Chavan SS, Tracey KJ, Bouton CE.** 2017, Proc Natl Acad Sci.

25. *Evidence-based guideline update: Vagus nerve stimulation for the treatment of epilepsy.* **George L. Morris III, David Gloss, Jeffrey Buchhalter, Kenneth J. Mack, Katherine Nickels, Cynthia Harden.** 2013, Neurology, Vol. 81, pp. 1453–1459.

26. *Cytokine-specific neurograms in the sensory vagus nerve.* **Steinberg BE, et al.** Bioelectron. Med., Vol. 3, pp. 7–17.

27. *Glucose-Sensitive Afferent Nerve Fibres in the Hepatic Branch of the Vagus Nerve in the Guinea-Pig.* **Niijima, Akira.** 1982, J. Physiol., Vol. 332, pp. 315-323.

28. **Tecnology, Tucker-Davis.** [Online] https://www.tdt.com/files/manuals/TDTSys3_Manual.pdf.

29. *The Use of Fast Fourier Transform for the Estimation ofPower Spectra: A Method Based on Time Averaging Over Short, Modified Periodograms.* **Welch, P. D.** 2, 1967, Transactions on Audio and Electroacoustics, Vol. 15.

30. *The EEG as potential mapping—the value of the average monopolar reference.* **Offner, F.F.** 1950, Electroencephalogr. Clin. Neurophysiol, Vol. 2, pp. 213-214.

31. *Manual Hematoxylin and Eosin Staining of Mouse Tissue Sections.* **Robert D. Cardiff, Claramae H. Miller, Robert J. Munn.** 2014, Cold Spring Harb Perspect Med.

32. *Hematoxylin and Eosin Staining of Tissue and Cell Sections.* **Andrew H. Fischer, Kenneth A. Jacobson, Jack Rose, Rolf Zeller.** 2008, Cold Spring Harb Perspect Med.

33. *Biofilm Detection With Hematoxylin-Eosin Staining.* **Christian J. Hochstim, Judy Yujin Choi, Derek Lowe, et al.** 5, 2010, Arch Otolaryngol Head Neck Surg, Vol. 136, pp. 453-456.

34. *The Wonderful Colors of the Hematoxylin–Eosin Stain in Diagnostic Surgical Pathology.* **Chan, John K. C.** 1, 2014, International Journal of Surgical Pathology, Vol. 22, pp. 12–32.

35. *Realizing flexible bioelectronic medicines for accessing the peripheral nerves–technology considerations.* **Serdijn, Giagka and.** 8, 2018, Bioelectronic Medicine, Vol. 4.

36. *Bioelectronic medicine: updates, challenges and paths forward.* **Tracey, Pavlov and.** 1, 2019, Bioelectronic Medicine, Vol. 5.

37. *A critical review of interfaces with the periferal nervous system for the control of neuroprostheses and hybrid bionic system.* **Xavier Navarro, Thilo B. Krueger, Natalia Lago, Silvestro Micera, Thomas stieglitz, Paolo Dario.** 2005, Journal of the Periferal Nervous System, Vol. 10, pp. 229-258.

38. *Update on Peripheral Nerve Electrodes for Closed-Loop Neuroprosthetics.* **Emil H. Rijnbeek, Nick Eleveld, Wouter Olthuis.** 350, 2018, Frontiers in Neuroscience, Vol. 12.

39. *A transverse intrafascicular multichannel electrode (TIME) to interface with the peripheral nerve.* **Tim Boretius, Jordi Badia, Aran Pascual-Font, Martin Schuettler, Xavier Navarro, Ken Yoshida, Thomas Stieglitz.** 2010, Biosensors and Bioelectronics, Vol. 26, pp. 62–69.

40. *Modelization of a self-opening peripheral neural interface: A feasibility study.* **Annarita Cutrone, Pier Nicola Sergi, Silvia Bossi, Silvestro Micera.** 10, 2011, Medical Engineering & Physics, Vol. 33, pp. 1254-1261.

41. *Polymers for Neural Implants.* **Hassler, C., Boretius, T., Stieglitz, T.** 2011, Journal of Polymer Science: Part B: Polymer Physics, Vol. 49, pp. 18–33.

42. *Elimination of electrocardiogram contamination from vagus nerve recordings using ICA.* **G. de Lannoy, T. Costecalde, J. Marin, M. Verleysen1, J. Delbeke.** Seoul, Korea : s.n., 2009. 14th Annual Conference of the International FES Society.

43. *Extracting wavelet based neural features from human intracortical recordings for neuroprosthetics applications.* **Mingming Zhang, Michael A. Schwemmer, Jordyn E. Ting, Connor E. Majstorovic, David A. Friedenberg, Marcia A. Bockbrader, W. Jerry Mysiw, Ali R. Rezai, Nicholas V. Annetta, Chad E. Bouton, Herbert S. Bresler, Gaurav Sharma.** 11, 2018, Bioelectronic Medicine, Vol. 4.

44. *Optimal ventricular rate slowing during atrial fibrillation by feedback AV nodal-selective vagal stimulation.* **Youhua Zhang, Kent A. Mowrey, Shaowei Zhuang, Don W.**

Wallick, Zoran B. Popović, Todor N. Mazgalev. 2002, Am J Physiol Heart Circ Physiol, Vol. 282, pp. 1102–1110.

45. *Electrophysiological Control of Ventricular Rate During Atrial Fibrillation.* **Matthew S. Waninger, Joe D. Bourland, Leslie A. Geddes, William E. Schoenlein, George Graber, Walter E. Weirigh, George R. Wodicka.** 2000, Pacing and clinical electrophysiology, Vol. 23, pp. 1239-1244.

46. *Sensory Neurons that Detect Stretch and Nutrients in the Digestive System.* **Erika K.Williams, Rui B.Chang, David E.Strochlic, Benjamin D.Umans, Bradford B.Lowell, Stephen D.Liberles.** 2016, Cell, Vol. 166, pp. 209–221.